Amino Acids (2015) 47:1135–1153
DOI 10.1007/s00726-015-1942-0

ORIGINAL ARTICLE

Radiolabeled new somatostatin analogs conjugated to DOMA chelator used as targeted tumor imaging agent: synthesis and radiobiological evaluation

Kakali De · Indranil Banerjee · Mridula Misra

Received: 23 November 2014 / Accepted: 14 February 2015 / Published online: 6 March 2015

Abstract Several receptor-specific radiopeptides have been developed and effective in the diagnosis of malignant diseases. Among them, somatostatin receptor (SSTR) scintigraphy with ^{111}In-DTPA-octreotide has become a tumor diagnostic radiopharmaceutical in nuclear medicine. However, it suffers some drawbacks concerning the imaging properties and elevated radiation burden of ^{111}In. Here, we report the synthesis of radiolabeled two new octapeptides with improved uptake in SSTR2-positive tumors in comparison with ^{99m}Tc-HYNIC-Tyr^3-octreotide (HYNIC-TOC). Octapeptides were synthesized in high yield by Fmoc solid-phase synthesis and coupling the macrocyclic chelator DOMA(1,4,7-Tri-Boc-10-(carboxymethyl)-1,4,7,10-tetraazocyclododecane-1-yl-monoacetic acid) to these peptides for ^{99m}Tc labeling. New peptides DOMA-Asn^3-octreotate(DOMA-AATE) and DOMA-Pro^3-octreotate(DOMA-PATE) were purified, characterized by RP-HPLC, MALDI-mass, ^{1}H-NMR, ^{13}C-NMR. Labeling was performed by $SnCl_2$ method to get products with excellent radiochemical purity (97 %). Radiopeptides were found to be substantially stable under physiological condition for 24 h. Internalization and receptor-binding studies were determined in somatostatin receptor-expressing C6-glioma cell line and rat brain cortex membrane and the results compared with HYNIC-TOC as standard. The IC_{50} values of ^{99m}Tc-DOMA-AATE(1.10 ± 0.48 nM) and ^{99m}Tc-DOMA-PATE(1.76 ± 0.06 nM) showed high affinity binding for SSTR2 receptor and they internalized rapidly in C6 cells. Biodistribution and imaging studies were performed in C6 tumor-bearing rat under gamma camera showing significant uptake in kidney, urine and C6 tumor. Radiopeptides exhibited fast blood clearance and rapid elimination through the urinary systems. However, ^{99m}Tc-DOMA-AATE exhibited the highest tumor to muscle and tumor to blood uptake ratios among three. These favorable characteristics validate ^{99m}Tc-DOMA-AATE as a more promising ^{99m}Tc-radiotracer than ^{99m}Tc-DOMA-PATE, ^{99m}Tc-HYNIC-TOC for SSTR2-positive tumor scintigraphy.

Keywords Somatostatin receptor · HYNIC · DOMA · Octreotide · ^{99m}Tc · C6 tumor

Introduction

Radiolabeled receptor-binding small peptides have emerged as an essential class of radiopharmaceutical that promises to dramatically change the field of nuclear medicine as imaging agent for detection of tumors, thrombosis as well as infection/inflammation (Fischman et al. 1993). Peptides can penetrate into tumors and possess binding affinities that are comparable with or even better than those of antibodies. Solid-phase peptide synthesis (SPSS) has been accepted as a prevailing tool in the generation of several biological important and chemically modified peptides (Arnold et al. 2000; Liu and Edwards 1999; Susini and Buscail 2006). Several human tumors overexpress receptors for the peptide hormone somatostatin (SST), which comprises five subtypes: SST(1–5) (Koenig et al. 1997; Kwekkeboom and Krenning 2002; Susini and Buscail 2006). The native hormone, however, is susceptible to rapid

Handling Editor: Michael Platten.

K. De (✉) · I. Banerjee · M. Misra
Division of Infectious Diseases and Immunology, Nuclear Medicine Department, Council of Scientific and Industrial Research (CSIR)-Indian Institute of Chemical Biology, 4 Raja S C Mullick Road, Kolkata 700032, West Bengal, India
e-mail: kakalide@yahoo.com; mridulamisra@iicb.res.in

enzymatic degradation ($t_{1/2}$ = 2.3 min in blood) and is, therefore, unsuitable for in vivo applications. For this purpose, long-lived small synthetic somatostatin analogs have been developed, such as octreotide, octreotate and their derivatives (Nikolopoulou et al. 2006; Gandomkar et al. 2007). Numerous studies have focused on improving the target tissue uptake of radiolabeled somatostatin analogs. It has also been shown that changing the C-terminus from an alcohol to a carboxylic acid and replacing the N-terminal D-Phe in octreotide with D-Tyr increase uptake of the peptide in somatostatin receptor subtype2 (SSTR2)-positive tissues (Li et al. 2002; Storch et al. 2005). Nowadays, radiolabeled somatostatin analogs have been clinically used, and ^{111}In-DTPA-octreotide (octreoscan) has been used for the localization and staging of SSTR2-positive neuroendocrine tumors (De Jong et al. 1998; Decristoforo et al. 2000; Li et al. 2002; Okarvi 2004; Storch et al. 2005). Despite the success of this compound as an imaging agent, octreoscan has two main obstacles to use, the first is the high cost, limited availability and suboptimal physical decay properties of ^{111}In. For these reasons, radiopharmaceuticals labeled with ^{99m}Tc are in demand both for economic reasons and the favorable imaging characteristics of technetium (γ energy of 140 keV and 6 h half-life) (De Jong et al. 1998; Decristoforo et al. 2000; Okarvi 2004; Graham and Menda 2011). So somatostatin analog incorporating ^{99m}Tc would be more desirable and has been pursued for tumor scintigraphic imaging in human. For in vivo scintigraphic studies by planner imaging or single photon emission computed tomography (SPECT), ^{99m}Tc is the radionuclide of choice by virtue of its superior nuclear properties, cost effectiveness and wide availability (De Jong et al. 1998; Decristoforo et al. 2000; Okarvi 2004; Graham and Menda 2011). In this regard, SSTR-positive peptide analogs radiolabeled with ^{99m}Tc are highly attractive than octreoscan for nuclear medicinal use. Over the last decades, various attempts have been developed to the preparation of ^{99m}Tc-labeled HYNIC (hydrazinonicotinamide)-conjugated somatostatin analogs for tumor imaging (Babich and Fischman 1995; Decristoforo and Mather 1999; Decristoforo et al. 2000). Here, we have used new bifunctional chelating agent derived from the macrocyclic 1,4,7-Tri-Boc-10-(carboxymethyl)-1,4,7,10-tetraazocyclododecane-1-yl-monoacetic acid (DOMA) for the preparation of ^{99m}Tc-labeled new SSTR2-positive stable and efficient somatostatin analogs.

In this manuscript, we present the synthesis and preclinical evaluation of novel synthetic somatostatin analogs such as DOMA-Asn^3-Octreotate (DOMA-AATE), DOMA-Pro3-Octreotate (DOMA-PATE) with regard to pharmacokinetic study, binding affinity, biodistribution and imaging studies in a C6 glioma tumor-bearing rat model and compare its biological properties with HYNIC-Tyr^3-octreotide (HYNIC-TOC) as potential tumor targeting agents.

Materials and methods

Reagents and instrumentation

All standard reagents, solvents and the chemicals were obtained from commercial sources and Fmoc-amino acids for the peptide synthesis, H-Thr(tBu)-(2-chlorotrityl)-resin, were purchased from Nova Biochem, USA. The macrocyclic chelator 1,4,7-Tri-Boc-10-carboxymethyl-1,4,7,10-tetraazocyclododecane-1-yl-acetic acid (DOMA) was purchased from Sigma Chemicals. DIEA was obtained from SRL, India. Piperidine, DMF, EDDA, tricine, $SnCl_2$, picryl sulfonic acid, thioanisole and acetaldehyde were obtained from Sigma Chemicals, USA. All other chemicals, solvents and silica gel plates were obtained from MERCK, Germany. The cell culture medium was Dulbecco's Modified Eagle's Medium (DMEM) supplemented with 10 % fetal bovine serum (FBS), amino acids, vitamins and penicillin/streptomycin from Gibco. ^{99m}Tc-sodium pertechnetate (Na[$^{99m}TcO_4^-$]) was obtained by 2-butanone extraction from a 5(N) NaOH solution of $^{99}MoO_4-$ (purchased from BARC, Mumbai, India) and technetium generator was obtained from the author's Indian Institute of Chemical Biology and used for radiopharmaceutical preparation. The cancer cell lines used in this study were C6 glioma cell line.

The Quantitative γ counting was performed on a well-type γ counter (γ-ray spectrometer: GRS 23C, ECIL, Hyderabad, India). Analytical reverse-phase HPLC was performed on Shimadzu RP-HPLC system equipped with μ bondapak C18, 10 μm, 125 Å, 7.8 × 300 mm reverse-phase column and UV detector (Shimadzu, Japan), set at 254 nm, using gradient solvent systems.

Solid-phase peptide synthesis

Two new octreotide analogs DOMA-Asn^3-Octreotate (DOMA-AATE), DOMA-Pro^3-Octreotate (DOMA-PATE), and HYNIC-Tyr^3-octreotide (HYNIC-TOC) were synthesized by standard Fmoc solid-phase synthesis (SPPS) (Kwekkeboom and Krenning 2002; Panwar et al.2005; Gandomkar et al. 2007) on acid sensitive H-Thr(tBu)-(2-chlorotrityl) resin for DOMA-AATE, DOMA-PATE and O-*t*-butylthreoninol-(2-chlorotrityl) resin for HYNIC-TOC. The amino acid sequence of the peptides Asn^3-octreotate was D-Phe-Cys-Asn-(D)Trp-Lys-Thr-Cys-Thr-OH, Pro^3-octreotate was D-Phe-Cys-Pro-Trp-Lys-Thr-Cys-Thr-OH and for Tyr^3-octreotide was D-Phe-Cys-Tyr-(D)Trp-Lys-Thr-Cys-Thr-OH. For this peptide synthesis, at first resin (0.1 mmol) was treated with 20 % piperidine in DMF under nitrogen atmosphere (10 min) to remove the Fmoc group. The resin was thoroughly washed with DMF. Fmoc-protected amino acids were activated in situ in AA cartridges with TBTU/DIPEA in DMF. Coupling of each amino acid

was performed in the presence of 5 mol excess of Fmoc-amino acid (0.5 mmol), 0.5 mmol TBTU, and 1 mmol DIPEA in DMF (3 ml). Amino acids were coupled by removing Fmoc-protecting groups with 20 % piperidine/DMF for 10 min followed by washing with DMF. The complete synthesis was achieved by stepwise coupling of Fmoc-amino acids to the growing peptide chain on the resin. Progress of the amino acid coupling was monitored by color change of picryl sulfonic acid (TNBS). This process was repeated until the required sequence was achieved. Finally, coupling of prochelator to peptide for DOMA-AATE and DOMA-PATE was performed in the presence of 5 mol excess of macrocyclic chelator DOMA (1,4,7-Tri-Boc-10-(carboxymethyl)-1,4,7,10-tetraazocyclododecane-1-yl)-acetic acid) and for HYNIC-TOC, 5 mol excess of BOC-HYNIC, and 4.5 mol excess of TBTU and 10 mol excess of DIPEA in DMF for 40 min; coupling success was checked by TNBS test. The coupled resin was filtered and rinsed with DMF. The average coupling yield was calculated from the increase in weight of the elongated peptide resin divided by the weight of protected peptide.

Disulfide bond formation and cleavage of peptides from resin along with global deprotection

After that peptide chain was cyclized by the formation of Cys–Cys disulfide bond in solid phase (Lee et al. 1998; Kwekkeboom and Krenning 2002). A part (150 mg) of the peptide resin was swelled in DMF for 2 h at 25−30 °C. Then, this peptide resin solution was added dropwise to a vigorously stirred solution of 10-eq iodine (70 mg) in DMF. After a reaction time of 2 h at 25−30 °C, excess iodine was washed with DMF to remove the iodine color, and the resin was washed with ether and dried. The S–S cyclized peptide chain with all protecting groups was cleaved after treatment with 88 % TFA, 3 % thioanisole, 4 % ethane dithiol (EDT), 3 % triethyl silane (TIS) and 2 % water at 25 °C for 3–4 h. Then, it was rinsed with DMF and the crude product of DOMA-AATE and DOMA-PATE was precipitated with cold diethyl ether. Similarly, after peptide chain cyclization HYNIC-TOC was precipitated with cold diethyl ether.

Purification of peptide (DOMA-AATE, DOMA-PATE and HYNIC-TOC)

Finally, the synthesized crude peptides DOMA-AATE, DOMA-PATE and HYNIC-TOC were purified and analyzed on a Shimadzu semi-preparative HPLC system, consisting of two LC20AD solvent pumps and an SPD-M20A prominenance diode array detector. Injections of 200 µL were eluted at a flow rate of 1 ml/min from a μ bondapack C-18, 10 µm, 125 Å, 7.8 × 300 mm reverse-phase column, using a gradient system consisting of 0.1 % TFA in water (solvent A) and 0.085 % TFA in acetonitrile (solvent B) was used. A 32 min binary gradient was used. Gradient I: 0 min 100 % A (0 % B), 5 min 80 % A (20 % B), 10 min 65 % A (35 % B), 15 min 50 % A (50 % B), 25 min 20 % A (80 % B), 30 min 0 % A (100 % B), 32 min 100 % A (0 % B). The column effluent was monitored using a UV detector set at 254 nm. The major isolated peaks for all the peptides were collected. After that, isolated peaks were lyophilized and stored at −20 °C freezer. Finally, the purified DOMA-AATE, DOMA-PATE and HYNIC-TOC were characterized by matrix-assisted laser desorption ionization (MALDI) spectrometry in positive-ion mode and the structure of the peptides was then elucidated by analytical HPLC, ^{1}H NMR, and FT-IR.

Radiolabeling of the peptides and quality control

Radiolabeling (Lee et al. 1998; Storch et al. 2005; Guggenberg et al. 2006; De et al. 2012) of DOMA conjugate peptides DOMA-AATE, DOMA-PATE and HYNIC conjugate peptide HYNIC-TOC with ^{99m}Tc was performed using a freshly prepared solution of stannous chloride dihydrate $SnCl_2.2H_2O$ (25 µg) as reducing agent. In the case of DOMA-AATE and DOMA-PATE, stannous ion was added from fresh 0.5 mg ml^{-1} solution of stannous chloride in 10 mM HCl to various activities of ^{99m}Tc (37–370 MBq) and incubated at room temperature (22 °C) for 30 min. In case of HYNIC-TOC, radiolabeling with ^{99m}Tc was performed using stannous ion, ^{99m}Tc (37–370 MBq) and EDDA (10 mg in 0.5 ml 0.1 N NaOH), tricine (20 mg in 5 ml distilled water), as coligands to stabilize ^{99m}Tc bound to the hydrazine residue of the peptide conjugates (20 µg). Then, the labeling solution was incubated for 15–20 min at 100 °C. In all the cases, final pH of the labeling solution was adjusted to 7–8. At the end of the incubation time, after cooling to room temperature the relative front (R_f) values and radiolabeling yield of radiolabeled component were calculated using thin-layer radio chromatography (TLRC) method. After cooling to room temperature, the radiochemical purity assessment and quality control of the labeled peptide were achieved by RP-HPLC and instant thin-layer chromatography on silica gel plates (ITLC-SG). HPLC technique was used to validate ITLC approach. The radiochemical purity of ^{99m}Tc-DOMA-AATE/^{99m}Tc-DOMA-PATE/^{99m}Tc-HYNIC-TOC was determined by RP-HPLC with reversed-phase C18 column (4.6 mm x 250 mm, μ bondapak column from waters). The mobile phase used in RP-HPLC for gradient system consists of 0.1 % TFA/water (solvent A) and 0.85 % TFA/acetonitrile (solvent B) at a 1 mL/min flow rate. Gradient II: 0 min 100 % A (0 % B), 2 min 90 % A (10 % B), 6 min 80 % A (20 % B), 12 min 50 % A (50 % B), 25 min 10 % A (90 % B), 35 min 90 % A (10 % B), 45 min 100 % A (0 % B). ITLC-SG was

performed using different mobile phases. 2-butanone was used to determine the amount of free $^{99m}TcO_4^-$ ($R_f = 1$), 0.1 M sodium citrate of pH 5 was used to determine the non-peptide bound ^{99m}Tc-coligand and $^{99m}TcO_4^-$ ($R_f = 1$), and methanol/1 M ammonium acetate 1/1 was used for ^{99m}Tc-colloid ($R_f = 0$). The radiochemical purity of ^{99m}Tc-HYNIC-TOC was determined by RP-HPLC and ITLC method in the same way.

Stability studies

The in vitro stability of the ^{99m}Tc-DOMA-AATE/^{99m}Tc-DOMA-PATE/^{99m}Tc-HYNIC-TOC complex was studied separately in phosphate buffer saline (PBS at pH 7.4), and freshly collected rat serum for 1–6 h at room temperature (Behera et al. 2011; Hanaoka et al. 2009). To an aliquot (0.1 ml) of the radiolabeled complex ^{99m}Tc-DOMA-AATE/^{99m}Tc-DOMA-PATE/^{99m}Tc-HYNIC-TOC, either saline (0.9 ml) or serum (0.9 ml) was added, and the mixtures were incubated at 37 °C for 24 h. After incubation, samples were withdrawn from the mixture and analyzed by ITLC at 0, 1, 3, 4, and 24 h of incubation period. For the solution of rat serum, the aliquot was added to 100 µL of 50 % trifluoroacetic acid (TFA). After centrifugation, the supernatant was taken for ITLC analysis and then 10 µL of this mixture was taken at each time point, added to a strip ITLC and the percentage of ^{99m}Tc-DOMA-AATE/^{99m}Tc-DOMA-PATE/^{99m}Tc-HYNIC-TOC was determined using gamma counter. The stability of radiolabeled peptides was also validated by RP-HPLC using gradient II as solvent system at different time intervals.

Partition coefficient determination

The octanol–buffer partition coefficient was measured using a standard protocol (De et al. 2010, 2012). The partition coefficient was determined by mixing the ^{99m}Tc-DOMA-AATE/^{99m}Tc-DOMA-PATE complex (100 µL) with an equal volume (2 mL) of 1-octanol and phosphate buffer (0.025 M, pH 7.4) in a centrifuge tube. The mixture was vortexed at room temperature for 2 min and then centrifuged at 5000 rpm for 5 min to ensure complete separation of layers. The two layers were separated and from each phase 0.1 mL of the aliquot was removed and counted separately in a well γ-counter. The ratio of octanol layer counts to aqueous layer counts was expressed as a partition coefficient (p) and log p was used for the determination of lipophilicity of the complex. Care was taken to avoid cross contamination between the two phases. The partition coefficient of ^{99m}Tc-HYNIC-TOC was also determined by the same way.

p = (cpm in octanol − cpm in background)/(cpm in buffer − cpm in background).

Plasma protein binding assay

For this experiment, ^{99m}Tc-DOMA-AATE/^{99m}Tc-DOMA-PATE/^{99m}Tc-HYNIC-TOC (100 µL) was mixed with the fresh rat plasma (100 µL) in the centrifuge tube. Now, the mixture was incubated at 37 °C for 2 h, and the plasma protein was precipitated by adding 1 ml trichloroacetic acid (10 %) to the mixture. The supernatant and precipitate were separated by centrifugation at 3000 rpm for 5 min. The radioactivities of both the phases were measured separately. The above experimental procedure (De et al. 2010, 2012) was repeated three times. The percentage of protein binding was determined by the following equation:

$$\text{Plasma protein binding } \% = \left(\text{Precipitate counts (CPM)}\Big/\left[\text{Precipitate Counts (CPM)} + \text{Plasma Counts (CPM)}\right]\right) \times 100\,\%.$$

Blood clearance study in rat

The study of blood (Decristoforo et al. 2000; De et al. 2010, 2012) clearance was performed in anaesthetized well-hydrated Sprauge–Dawley (SD) rats. The ^{99m}Tc-DOMA-AATE/^{99m}Tc-DOMA-PATE/^{99m}Tc-HYNIC-TOC (1 mCi, 0.2 ml) was administered to the rat via intravenous injection through pre-cannulated femoral vein. A series of blood samples (20 µL) were withdrawn from the other femoral vein in the tube at different time intervals (2, 5, 15, 30, 60, 90 and 120 min), counted in GRS (gamma-counter), and weighed accurately. The radioactivity of the withdrawn blood was expressed as percentage of injected dose/g (%ID/g) of blood sample at each time and plotted against respective time interval to obtain the blood clearance curve of the radiopharmaceuticals.

Cell culture

The rat C6 glioma cells were brought from National Centre for Cell Science, Pune, India and cell was grown confluent in DMEM supplemented with 10 % FBS, 100 µg mL^{-1} streptomycin and 100 UI mL^{-1} penicillin in a humidified incubator at 37 °C with 5 % CO_2: 95 % air. Culture medium was replenished 2–3 days after seeding and every other day thereafter, unless otherwise noted. Subculturing was performed employing a trypsin/EDTA (0.05/0.02 % w/v) solution (De et al. 2012).

Receptor-binding study

The binding affinity of DOMA-AATE/DOMA-PATE was performed in a competition binding assay (Nikolopoulou et al. 2006; Maina et al. 2006; Gandomkar et al. 2007; De et al. 2012) against ^{99m}Tc-HYNIC-TOC as the radioligand.

Similar competition binding assay was performed for HYNIC-TOC. It is reported earlier that C6 glioma cells have overexpression of the SSTR2 (De et al. 2012). Here C6 glioma cell membranes and rat brain cortex membrane homogenates were used as a source of SSTR2. Both the membrane preparations were performed according to a published method (Gandomkar et al. 2007; De et al. 2012) and the protein concentration of the membrane samples was determined by Bradford reagent (Biorad) using bovine serum albumin as the standard. Typically, 50,000 cpm of radioligand was added in each test tube, containing rat brain cortex (corresponding to 50 μg protein) or C6 cell membrane homogenates (corresponding to 10 μg protein) in the presence of increasing amounts of DOMA-AATE/DOMA-PATE peptide in a total volume of 300 μL of 50 mM HEPES (pH 7.6, 0.3 % BSA, 5 mM $MgCl_2$, 10 μM bacitracin). The samples were incubated in triplicate for 40 min at 37 °C and incubation was terminated by addition of ice-cold buffer (1 mL, 10 mM HEPES, 150 mM NaCl, pH 7.6). The suspension was rapidly filtered over glass fiber filters (Whatman GF/B presoaked in binding buffer) and the filters were rinsed thoroughly with buffer (4 × 2 mL) and filter activity was measured on a gamma counter. Inhibitory concentrations of 50 % binding (IC_{50}) values were calculated using non-linear regression with version 6.0 Origin software.

Radioligand internalization study

Internalization experiments were performed using C6 cells seeded at a density of 8–9 × 10^5 cells per well in six-well plates and grown to confluence for 48 h. On the day of the experiment, cells were washed twice with ice-cold internalization medium prepared with DMEM nutrient mixture supplemented by 1 % (v/v) FBS (Nikolopoulou et al. 2006; Maina et al. 2006; Gandomkar et al. 2007; De et al. 2012). Furthermore, 1 mL of internalization buffer was added to each well and the plates were incubated at 37 °C for about 1 h. Afterward, approximately 300,000 cpm ^{99m}Tc-DOMA-AATE/^{99m}Tc-DOMA-PATE/^{99m}Tc-HYNIC-TOC (150 μL, 2.5 pmol per well) were added to the medium and the cells were incubated at 37 °C in triplicates for each time point of 2, 5, 15, 30, 60 and 120 min incubation. To determine non-specific membrane binding and internalization, cells were incubated with radioligand in the presence of 10 μM HYNIC-TOC. The cellular uptake was stopped at appropriate time periods by removing medium from the cells and washing twice with 1 ml of ice-cold PBS. An acid wash for 10 min with a 0.1 M glycine buffer (pH 2.8) on ice was also performed twice. Finally, the cells were treated with 1 N NaOH. The culture medium and the receptor bound and internalized fractions were measured radiometrically in a gamma counter.

Tumor implantation in animals

Female Sprague–Dawley (SD) rats weighing 100–150 gm were housed under aseptic conditions, which included filtered air and sterilized food, water, bedding and cages. All the animal experiments were performed in compliance with the approval of the Institutional Animal Ethics Committee of CSIR-Indian Institute of Chemical Biology, Kolkata, India.

C6 rat glioma tumor cells (5–10 × 10^6 cells) freshly suspended in sterile PBS were injected subcutaneously into the flank of 6-week-old SD rats (100–150 gm). 21 days after inoculation, a solid palpable tumor mass (tumor weight 0.4–0.7 g) was observed and the C6 glioma tumor-bearing rat was used for further experiments.

Biodistribution study on tumor-bearing rats

Biodistribution studies (Nikolopoulou et al. 2006; Maina et al. 2006; Gandomkar et al. 2007; De et al. 2012) were performed in glioma tumor-bearing SD rat. Rats were anesthetized with an intraperitoneal injection of a 50 mg kg^{-1} ketamine and well hydrated by intraperitoneal administration of saline (0.9 %, 2 ml) for 1 h. After that under anesthesia rats were injected with 20 MBq of 0.35 nmol (0.5 μg total peptide mass) ^{99m}Tc-DOMA-AATE/^{99m}Tc-DOMA-PATE/^{99m}Tc-HYNIC-TOC in saline separately into the femoral vein. To determine the non-specific uptake of the radioligand, we injected another group of rats with 100 μg HYNIC-TOC in 50 μL saline as a co-injection with the radioligands. After preset time intervals (10, 30, 60 and 120 min), the animals were killed by intravenous injection of air. Immediately after killing, blood and urine samples were collected by puncture of heart and urinary bladder, respectively. Other organs (heart, liver, lung, spleen, blood, muscle, kidney, stomach, intestines, pancreas and tumor) were removed, rinsed with saline and blotted dry to remove the residual blood. After that, organs were carefully transferred into counting vials and weighed on a clinical scale and then radioactivity of the organs and the standards was counted in a double-channel well-type GRS (gamma-ray spectrometer: GRS 23C, ECIL) counter. Counts were corrected for background radiation and physical decay of the radioactivity. The uptake was expressed in percentage of injected dose per gram of each organ (%ID/g). Tumor to organ ratios was also calculated. Data were analyzed statistically by the *t* test, with the level of significance set at $P < 0.05$.

Tumor imaging by gamma scintigraphy

^{99m}Tc labeled DOMA-conjugated peptides ^{99m}Tc-DOMA-AATE/^{99m}Tc-DOMA-PATE and ^{99m}Tc-HYNIC-TOC

(500 μCi/500 μL) alone or together with 100 μg HYNIC-TOC (blocked animal) were administered intravenously through the femoral vein of the well-hydrated anaesthetized glioma tumor-bearing rats and placed under the head of an experimental γ-camera (Nikolopoulou et al. 2006; Maina et al. 2006; Gandomkar et al. 2007; De et al. 2012). Whole body images were taken using a gamma camera fitted with a low-energy parallel hole high-resolution all-purpose collimator at different time intervals up to 60 min. Imaging studies were performed at Thakurpukur Cancer Research center (Regional Radiation Medicine Centre, VECC, Kolkata) under Gamma Camera (GE Hawkeys). Image data were analyzed using the dynamic procedure of the Xeleris functional imaging workstation.

Statistical analyses

Data were expressed as means ± standard deviations for internalization and biodistribution was performed on origin software. Results were statistically analyzed using the Student's *t* test. Differences at the 95 % confidence level ($P < 0.05$) were considered statistically significant.

Results

Synthesis and characterization

Two new octapeptides DOMA-AATE and DOMA-PATE and another one HYNIC-TOC were synthesized by standard solid-phase method in the manual mode using side chain-protected Fmoc-conjugated amino acids and the TBTU/DIPEA coupling strategy. Peptide sequences assembled on H-Thr(tBu)-(2-chlorotrityl) resin for DOMA-AATE and DOMA-PATE (Fig. 1a, b) and on O-*t*-butyl-threoninol-(2-chlorotrityl) resin for HYNIC-TOC peptide (Fig. 1c) were synthesized employing Fmoc chemistry and the TBTU/DIPEA coupling strategy. We envisioned a synthetic route in which all steps would be done while the peptide was still attached to the solid support (Scheme 1), which would minimize losses from handling and successive preparative HPLC purifications. All the peptides DOMA-AATE, DOMA-PATE and HYNIC-TOC were purified by HPLC on C18 reverse-phase column (gradient elution with CH_3CN/H_2O). After lyophilization, they were obtained as white powders, in yields ranging from 55 to 60 %. The composition and structural identity of DOMA-AATE, DOMA-PATE and HYNIC-TOC were verified by HPLC chromatogram, ^{1}H NMR and MALDI-MS spectra. After HPLC purification, the purity of DOMA-AATE, DOMA-PATE and HYNIC-TOC was greater than 97 % as confirmed by HPLC method. The molecular mass of DOMA-AATE measured by MALDI-MS was 1211.56 *m/z* $(M + H)^+$ (calculated mass = 1212.44) (Fig. 2a), for DOMA-PATE *m/z* $(M + H)^+$ = 1195.68 (calculated mass = 1194.57) (Fig. 2b) and *m/z* $(M + H)^+$ = 1170.36 (calculated mass = 1170.96) for HYNIC-TOC (Fig. 2c). The HPLC retention time was 17.91 min for DOMA-AATE, 19.45 min for DOMA-PATE and 21.26 min for HYNIC-TOC.

^{1}H NMR spectrum of DOMA-AATE in D_2O showed peaks for two methyl groups of two threonine residues (δ = 1.16, 1.21), eighteen $-CH_2$ groups (δ = 2.48, 2.65, 2.67, 2.67, 2.67, 2.67, 2.65, 2.48, 3.25, 2.92-3.17, 3.18–2.93, 2.81–2.56, 3.06–2.81, 1.79, 1.29, 1.55, 2.67, 3.18–2.93), nine aromatic −CH protons (δ = 7.12, 7.16, 7.21, 7.27, 7.08, 7.18, 7.20, 7.22, 7.24) and eleven proton resonances (δ 4.92, 4.81, 4.76, 4.92, 6.80, 4.53, 4.61, 4.24, 4.81, 4.54, 4.34), which were indicative of α-protons of amino acid residue. The presence of four-quaternary carbon and ten carbonyl carbons was indicated by the ^{13}C NMR spectra. The IR absorption bands were characteristic of amino (3298 cm^{-1}) and amide carbonyl groups (1664 cm^{-1}).

The ^{1}H NMR spectrum of DOMA-PATE in D_2O showed peaks for two methyl groups of two threonine residues (δ = 1.15, 1.18), twenty $-CH_2$ groups (δ = 2.44, 2.63, 2.59, 2.59, 2.64, 2.64, 2.60, 2.42, 3.25, 2.90–3.28, 2.83–2.88, 2.09–2.34, 1.92–2.02, 3.41–3.51, 3.12–3.20, 1.61, 1.31, 1.45, 2.64, 2.92–3.14), nine aromatic –CH protons (δ = 7.10, 7.14, 7.28, 7.30, 7.13, 7.24, 7.28, 7.26, 7.26) and eleven proton resonances (δ = 4.86, 4.88, 4.40, 4.56, 7.12, 4.29, 4.38, 4.33, 5.11, 4.48, 4.26), which were indicative of α-protons of amino acid residues. The presence of four-quaternary carbon and nine carbonyl carbons was indicated by the ^{13}C NMR spectra. The IR absorption bands were characteristic of amino (3294 cm^{-1}) and amide carbonyl groups (1660 cm^{-1}).

The ^{1}H NMR spectrum of HYNIC-TOC in D_2O showed peaks for two methyl groups of two threonine residues (δ = 1.14, 1.22), nine $-CH_2$ groups (δ = 3.16, 2.82–2.85, 2.92–3.17, 2.89–2.93, 1.53, 1.39, 1.42, 2.74, 2.95–3.01), fifteen aromatic −CH protons (δ = 8.03, 6.97, 8.69, 7.36, 7.39, 7.29, 7.33, 7.47, 6.95, 6.92, 6.68, 6.64, 7.24, 7.11, 7.28) and nine proton resonances (δ = 4.92, 4.59, 7.18, 3.99, 4.34, 4.36, 4.32, 4.41, 4.27), which were indicative of α-protons of amino acid residues. The presence of eight-quaternary carbon and eight carbonyl carbons was indicated by the ^{13}C NMR spectra. The IR absorption bands were characteristic of amino (3287 cm^{-1}) and amide carbonyl groups (1664 cm^{-1}).

The IR, ^{1}H NMR spectra and mass spectral data of DOMA-AATE, DOMA-PATE and HYNIC-TOC supported the structure as given in Fig. 1a–c. The complete lists of ^{1}H NMR and ^{13}C NMR values are given in Table 1.

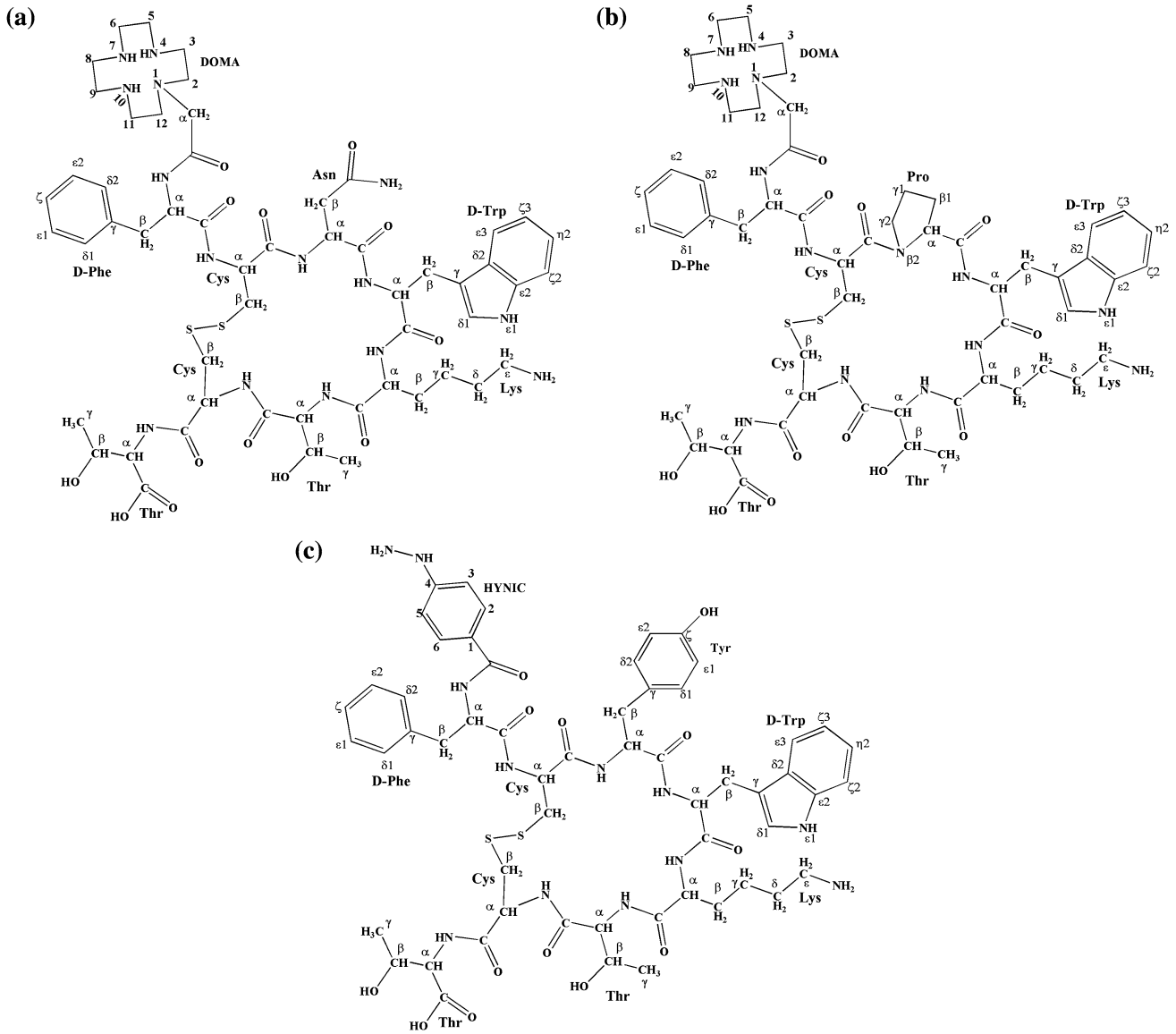

Fig. 1 **a** Structure of DOMA-Asn^3-octreotate (DOMA-AATE). **b** Structure of DOMA-Pro^3-octreotate (DOMA-PATE). **c** Structure of HYNIC-Tyr^3-octreotide (HYNIC-TOC)

Radiolabeling of the peptides

The purified peptides were successfully labeled with ^{99m}Tc. The radiolabeling efficiency, i.e., the percentage of the ^{99m}Tc-DOMA-AATE, ^{99m}Tc-DOMA-PATE and ^{99m}Tc-HYNIC-TOC in the preparation was more than 97 %, acquired via RP-HPLC and also ITLC. ITLC chromatograms did not show any changes in radiochemical purity during the time course considered for the analysis and the values were higher than 97 %. We obtained high radiochemical yield (97.48 ± 0.2 %) with very low amount of ^{99m}Tc-pertechnetate (0.5 ± 0.02 %), ^{99m}Tc-radiocolloid (0.32 ± 0.05 %) and ^{99m}Tc-coligand (1.5 ± 0.03 %). The radiochemical purity was further ascertained by RP-HPLC. In RP-HPLC analysis of ^{99m}Tc-DOMA-AATE and ^{99m}Tc-DOMA-PATE, we observed a single major peak at 13.50 and 14.25 min (retention time), (Fig. 3a, b) which was stable up to 24 h post-labeling period in the room temperature. In ITLC 2-Butanone solvent, the labeled ^{99m}Tc-DOMA-AATE, ^{99m}Tc-DOMA-PATE, ^{99m}Tc-coligands and ^{99m}Tc-colloid remain at the origin ($R_f = 0$) and ^{99m}Tc-pertechnetate moves at the solvent front ($R_f = 1$). For 0.1 M sodium citrate, pH 5.1 solvent system, the labeled ^{99m}Tc-DOMA-AATE and ^{99m}Tc-DOMA-PATE and ^{99m}Tc-colloid remain at origin ($R_f = 0$) and ^{99m}Tc-coligands and ^{99m}Tc-pertechnetate move at the solvent front ($R_f = 1$). For methanol/1 M ammonium acetate (1:1) solvent system, ^{99m}Tc-colloid remains at origin ($R_f = 0$) and labeled

Scheme 1 Solid-phase peptide synthesis of DOMA-AATE, DOMA-PATE and HYNIC-TOC

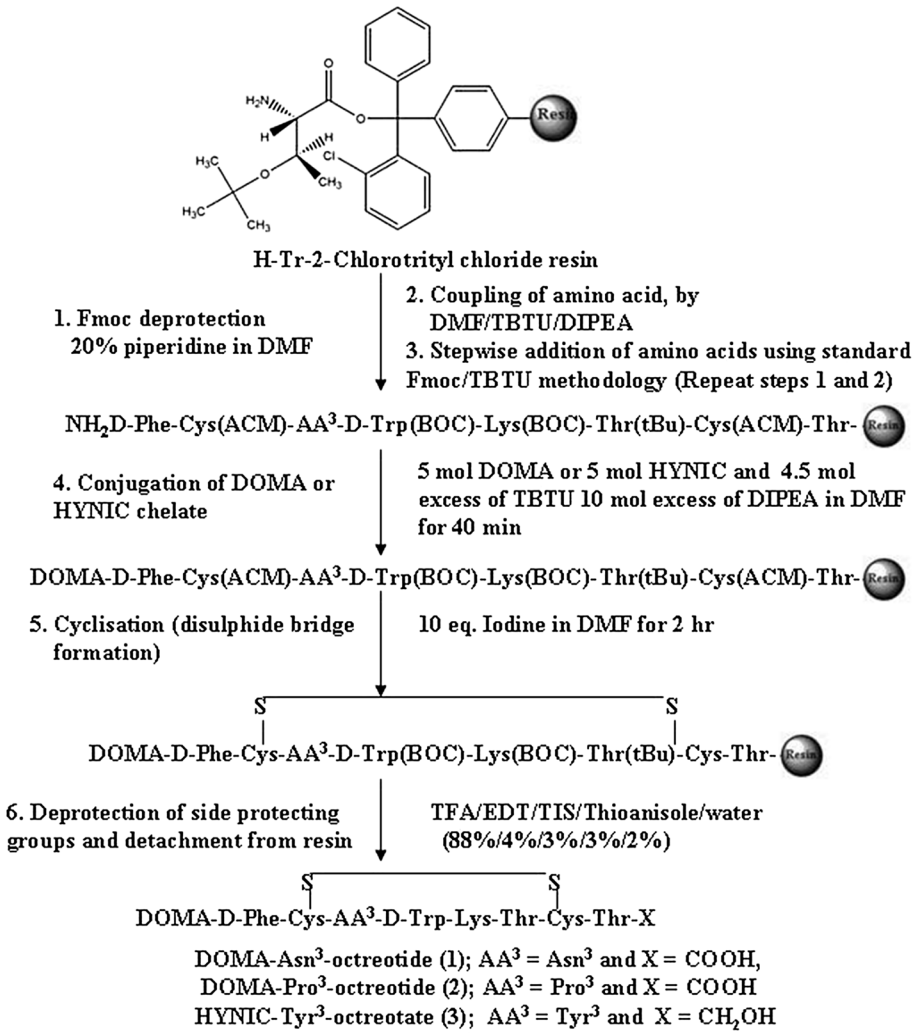

^{99m}Tc-DOMA-AATE and ^{99m}Tc-DOMA-PATE, ^{99m}Tc-coligands and ^{99m}Tc-pertechnetate move at the solvent front ($R_f = 1$). The probable energy minimized structure of ^{99m}Tc-DOMA-AATE, ^{99m}Tc-DOMA-PATE and ^{99m}Tc-HYNIC-TOC has shown in Fig. 4a–c. We expected this radiochemical complex structure from different literatures (Storch et al. 2005; Guggenberg et al. 2006; De et al. 2012) and MM2 energy minimized structure by energy minimization computation of all possible structures using Chem-3D ultra software (Fig. 4a, b). From the stability study, we found that ^{99m}Tc-DOMA-AATE and ^{99m}Tc-DOMA-PATE complexes were stable in PBS (pH 7.4) and FBS for 24 h post-labeling at room temperature (Decristoforo and Mather 1999). The results (Fig. 5) indicated that these complexes are stable enough for biodistribution and imaging studies.

^{99m}Tc-HYNIC-TOC was also purified by RP-HPLC and ITLC method like ^{99m}Tc-DOMA-AATE and ^{99m}Tc-DOMA-PATE. We observed a single major peak at 12.43 min (retention time) from RP-HPLC (Fig. 3c) that was also stable up to 24 h post-labeling periods in the room temperature (Fig. 5).

Partition coefficient (p) study

The octanol/buffer partition coefficient (log P) for the ^{99m}Tc-DOMA-AATE, ^{99m}Tc-DOMA-PATE and ^{99m}Tc-HYNIC-TOC complex was found to be -1.70 ± 0.12, -1.62 ± 0.10 and -1.15 ± 0.04 in PBS at pH 7.4. This implies that these radiocomplexes are hydrophilic in nature. The hydrophilicity of ^{99m}Tc-DOMA-AATE and ^{99m}Tc-DOMA-PATE is more than that ^{99m}Tc-HYNIC-TOC. The log P values are important parameters for the biological distribution of radiolabeled peptides.

Protein binding study

The percentage of plasma protein binding for ^{99m}Tc-DOMA-AATE and ^{99m}Tc-DOMA-PATE in blood plasma (SD rat) was 28.15 and 33 %, whereas the above value was

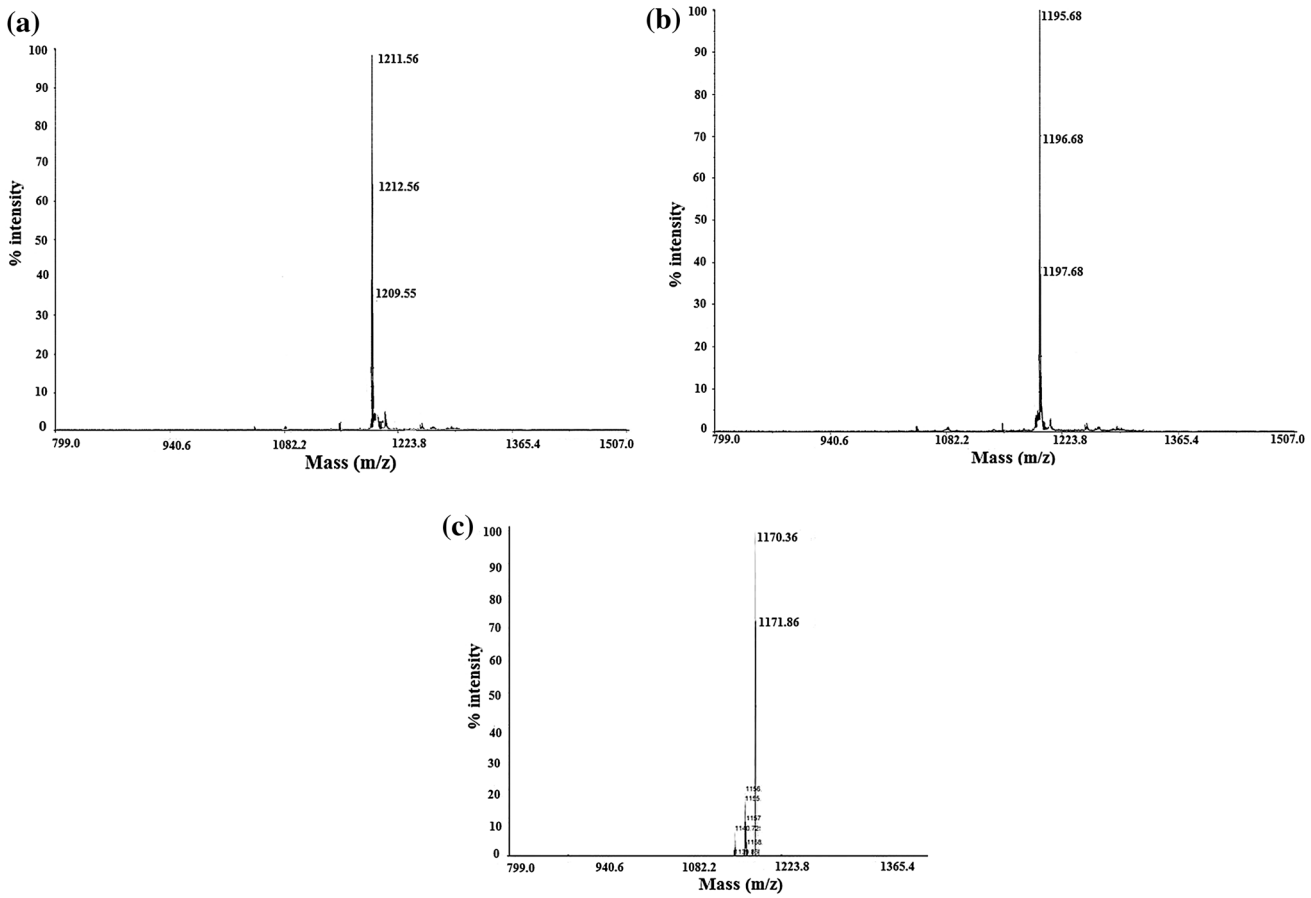

Fig. 2 **a** MALDI MS of DOMA-AATE. **b** MALDI MS of DOMA-PATE. **c** MALDI MS of HYNIC-TOC

46 % for ^{99m}Tc-HYNIC-TOC. These low protein binding values indicate that more of free drug is available for binding to the target. In general, the binding has significant influence on the tumor uptake in the biodistribution.

Receptor-binding studies and internalization

Competition binding experiments were performed in membrane homogenates from rat C6 glioma cells/from rat brain cortex, predominantly expressing SSTR2 (Lamszus et al. 1997; Barbieri and Florio 2011; De et al. 2012) (Fig. 6). Here we have shown the results of receptor-binding studies (membrane homogenates from rat C6 glioma cells) in Fig. 7. ^{99m}Tc-HYNIC-TOC was used as the radioligand while HYNIC-TOC was the reference compound. The IC_{50} values determined for DOMA-AATE and DOMA-PATE were 1.10 ± 0.48 and 1.76 ± 0.06 nM whereas the values calculated for the control compounds HYNIC-TOC were 2.97 ± 1.2 nM. In both the cases, the displacement studies revealed that DOMA-AATE and DOMA-PATE when compared with HYNIC-TOC inhibited the binding of ^{99m}Tc-HYNIC-TOC in a monophasic manner. Competition binding curves are shown in Fig. 6, demonstrating that DOMA-AATE and DOMA-PATE have higher affinity to SSTR2 than the binding affinity of HYNIC-TOC to SSTR2.

The C6 glioma tumor cell line is known to express SSTR2 receptor in vivo and in vitro (Lamszus et al. 1997; Barbieri and Florio 2011). The results with respect to the time-dependent internalization of ^{99m}Tc-DOMA-AATE and ^{99m}Tc-DOMA-PATE into C6 glioma cells during a 120 min incubation period at 37 °C are shown in Fig. 8. The cells were incubated at 37 °C with the radioligand ^{99m}Tc-DOMA-AATE/^{99m}Tc-DOMA-PATE with or without addition of a high excess of HYNIC-TOC (non-specific series). Radioactivity bound to the receptor on the membrane was "acid washed" with glycine buffer, pH 2.8 (membrane bound activity), whereas radioactivity in the cell (internalized activity) was collected after lysing the cells by treatment with 1 N NaOH. The curve of percent internalized activity versus the selected time points could be drawn (Fig. 7), revealing that ^{99m}Tc-DOMA-AATE and ^{99m}Tc-DOMA-PATE rapidly reached an internalization plateau of 85 % within the first 15 min of incubation in C6 cells. The

Table 1 ^{1}H and ^{13}C chemical shifts (ppm) for DOMA-AATE, DOMA-PATE and HYNIC-TOC in D_2O (600 MHz)

Residue	Position	DOMA-AATE		DOMA-PATE		HYNIC-TOC	
		^{1}H	^{13}C	^{1}H	^{13}C	^{1}H	^{13}C
DOMA	12	2.48	54.5 (CH_2)	2.44	51.8 (CH_2)	–	–
	11	2.65	43.2 (CH_2)	2.63	42.2 (CH_2)	–	–
	9	2.67	46.1 (CH_2)	2.59	44.1 (CH_2)	–	–
	8	2.67	46.1 (CH_2)	2.59	44.1 (CH_2)	–	–
	6	2.67	46.1 (CH_2)	2.64	48.1 (CH_2)	–	–
	5	2.67	46.1 (CH_2)	2.64	48.1 (CH_2)	–	–
	3	2.65	43.2 (CH_2)	2.60	40.2 (CH_2)	–	–
	2	2.48	54.5 (CH_2)	2.42	57.5 (CH_2)	–	–
	α	3.25	56.7 (CH_2)	3.25	56.2 (CH_2)	–	–
	CO	–	170.8 (C)	–	170.8 (C)	–	–
HYNIC	6	–	–	–	–	8.03	141.8 (CH)
	5	–	–	–	–	6.97	112.8 (CH)
	4	–	–	–	–	–	156.9 (C)
	2	–	–	–	–	8.69	138.6 (CH)
	1	–	–	–	–	–	120.4 (C)
	CO	–	–	–	–	–	167.2 (C)
D-Phe	α	4.92	52.9 (CH)	4.86	57.0 (CH)	4.96	56.4 (CH)
	β	3.17; 2.92	37.6 (CH_2)	3.28; 2.90	39.4 (CH_2)	3.16	39.2 (CH_2)
	γ	–	139.5 (C)	–	137.8 (C)	–	137.2 (C)
	δ1, δ2	7.12; 7.16	127.8 (CH)	7.10; 7.14	130.6 (CH)	7.36; 7.39	130.6 (CH)
	ε1, ε2	7.21; 7.27	128.7 (CH)	7.28; 7.30	130.3 (CH)	7.29; 7.33	128.8 (CH)
	ζ	7.08	126.0 (CH)	7.13	129.7 (CH)	7.47	127.3 (CH)
	CO	–	171.8 (C)	–	174.8 (C)	–	174.9 (C)
Cys	α	4.81	56.5 (CH)	4.88	54.8 (CH)	4.28	55.8 (CH)
	β	3.18; 2.93	38.6 (CH_2)	2.83; 2.88	44.0 (CH_2)	2.82; 2.85	41.2 (CH_2_
	CO	–	175.4 (C)	–	172.4 (C)	–	172.3 (C)
Asn	α	4.76	51.8 (CH)	–	–	–	–
	β	2.81; 2.56	37.5 (CH_2)	–	–	–	–
	CO (α)	–	175.4 (C)	–	–	–	–
	CO (β)	–	174.6 (C)	–	–	–	–
Pro	α	–	–	4.40	60.8 (CH)	–	–
	β 1	–	–	2.34; 2.09	29.5 (CH2)	–	–
	γ1	–	–	2.02; 1.92	22.2 (CH2)	–	–
	γ2	–	–	3.51; 3.41	45.6 (CH2)	–	–
	CO	–	–	–	174.7 (C)	–	–
Tyr	α	–	–	–	–	4.92	52.6 (CH)
	β	–	–	–	–	3.17; 2.92	29.4 (CH_2)
	γ	–	–	–	–	–	117.3 (C)
	δ1 δ2	–	–	–	–	6.95; 6.92	129.2 (CH)
	ε1, ε2	–	–	–	–	6.68; 6.64	124.3 (CH)
	ζ	–	–	–	–	–	127.9 (C)
	CO	–	–	–	–	–	174.6 (C)
D-Trp	α	4.92	58.8 (CH)	4.56	57.5 (CH)	4.59	55.7 (CH)
	β	3.06; 2.81	31.3 (CH_2)	3.12; 3.20	27.5 (CH_2)	2.89; 2.93	26.1 (CH_2)
	γ	–	110.9 (C)	–	109.7 (C)	–	108.1 (C)
	δ1	6.80	122.9(CH)	7.12	126.0 (CH)	7.18	126.6 (CH)
	δ2	–	127.5 (C)	–	123.3 (C)	–	115.3 (C)

Table 1 continued

Residue	Position	DOMA-AATE		DOMA-PATE		HYNIC-TOC	
		^{1}H	^{13}C	^{1}H	^{13}C	^{1}H	^{13}C
	$\varepsilon 2$	–	136.5 (C)	–	133.5 (C)	–	124.3 (C)
	$\eta 2$	7.18	120.1 (CH)	7.24	120.9 (CH)	7.24	121.9 (CH)
	$\varepsilon 3$	7.20	119.0 (CH)	7.28	119.9 (CH)	7.11	119.3 (CH)
	$\zeta 2$	7.22	111.1 (CH)	7.26	115.2 (CH)	7.28	136.0 (C)
	$\zeta 3$	7.24	122.2 (CH)	7.26	127.7 (CH)	7.28	118.8 (CH)
	CO	–	175.4 (C)	–	175.9 (C)	–	172.1 (C)
Lys	α	4.53	55.0 (CH)	4.29	55.3 (CH)	3.99	54.9 (CH)
	β	1.79	31.6 (CH_2)	1.61	31.1 (CH_2)	1.53	37.1 (CH_2)
	γ	1.29	20.7 (CH_2)	1.31	22.9 (CH_2)	1.39	21.4 (CH_2)
	δ	1.55	32.1 (CH_2)	1.45	27.5 (CH_2)	1.42	26.1 (CH_2)
	ε	2.67	42.1 (CH_2)	2.64	40.3 (CH_2)	2.74	38.8 (CH_2)
	CO	–	174.7 (C)	–	175.5 (C)	–	172.6 (C)
Thr	α	4.61	63.1 (CH)	4.38	61.6 (CH)	4.34	59.9 (CH)
	β	4.24	67.6 (CH)	4.33	69.1 (CH)	4.36	66.5 (CH)
	γ	1.21	18.9 (CH_3)	1.15	20.5 (CH_3)	1.14	18.7 (CH_3)
	CO	–	174.7 (C)	–	172.9 (C)	–	171.9 (C)
Cys	α	4.81	56.9 (CH)	5.11	53.9 (CH)	4.32	52.2 (CH)
	β	3.18; 2.93	38.6 (CH_2)	2.98; 3.14	42.3 (CH_2)	2.95; 3.01	38.8 (CH_2)
	CO	–	171.8 (C)	–	173.1 (C)	–	169.8 (C)
Thr	α	4.54	61.1 (CH)	4.48	60.8 (CH)	4.41	61.1 (CH)
	β	4.34	66.7 (CH)	4.26	68.3 (CH)	4.27	66.0 (CH)
	γ-CH_3	1.21	19.3 (CH_3)	1.18	20.5 (CH_3)	1.22	18.7 (CH_3)
	COOH	–	174.9 (C)	–	175.8 (C)	–	–

internalization was strongly reduced <15 % in the presence of excess cold peptide, and the process was receptor mediated.

Kinetics of blood clearance

The blood clearance curves of ^{99m}Tc-DOMA-AATE, ^{99m}Tc-DOMA-PATE and ^{99m}Tc-HYNIC-TOC have been shown in Fig. 8. Radioactivity in the blood was about 0.5 % of the injected dose/g (%ID/g) blood at 2 min post-injection. The radioactivity decreased to 0.02 % at 120 min post-injection. Retention in blood was low. The $T_{1/2}$ of the radiopharmaceuticals in blood was found at 30 min for ^{99m}Tc-DOMA-AATE. The blood clearance curve of these three radiocomplexes ^{99m}Tc-DOMA-AATE, ^{99m}Tc-DOMA-PATE and ^{99m}Tc-HYNIC-TOC showed very rapid clearance of radioactivity from the blood circulation at 10, 15 and 20 min and then it gradually decreases as shown in Fig. 8. The blood disappearance curve showed a biphasic pattern—an initial fast phase wherein approximately 50–60 % of activity was cleared within 10–20 min followed by slow phase in which the rate of excretion was comparatively less.

Biodistribution study

The results of the in vivo biodistribution studies in C6 glioma tumor-bearing SD rats at 10, 30, 60, and 120 min after intravenous administration of ^{99m}Tc-DOMA-AATE, ^{99m}Tc-DOMA-PATE and ^{99m}Tc-HYNIC-TOC separately are summarized in Table 2. The experiment was performed using five animals for each time point. Biodistribution studies with these radio peptides in glioma tumor-bearing rat were conducted to measure the localization of the radiopharmaceutical on tumors. The results are expressed as the percentage of the injected dose per gram of the organ (%ID/g). After administration of ^{99m}Tc-DOMA-AATE, ^{99m}Tc-DOMA-PATE and ^{99m}Tc-HYNIC-TOC maximum uptake of the radioactivity was observed in the kidney even at 30 min post-administration (PI) and was rapidly cleared from the blood and the body of rat into the urine via the kidney and urinary tract as a result of its high hydrophilicity. Results also showed that significant uptake was found in the SSTR-positive organs, including pancreas, intestines and C6 glioma tumor. The kidney uptake (%ID/g) of ^{99m}Tc-DOMA-AATE was 1.97 ± 0.11, 3.88 ± 0.21,

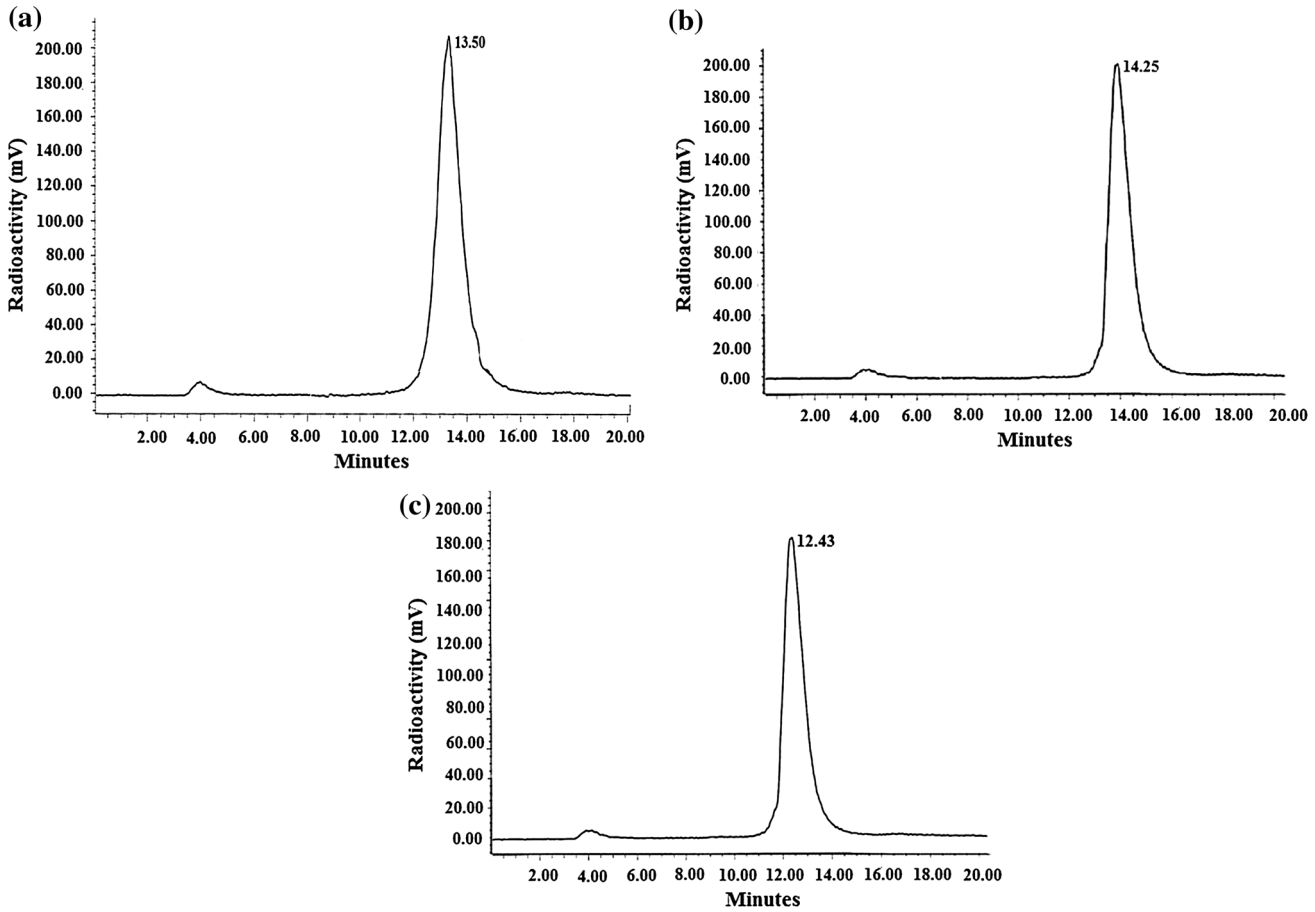

Fig. 3 **a** RP-HPLC chromatogram of ^{99m}Tc-DOMA-AATE. **b** RP-HPLC chromatogram of ^{99m}Tc-DOMA-PATE. **c** RP-HPLC chromatogram of ^{99m}Tc-HYNIC-TOC

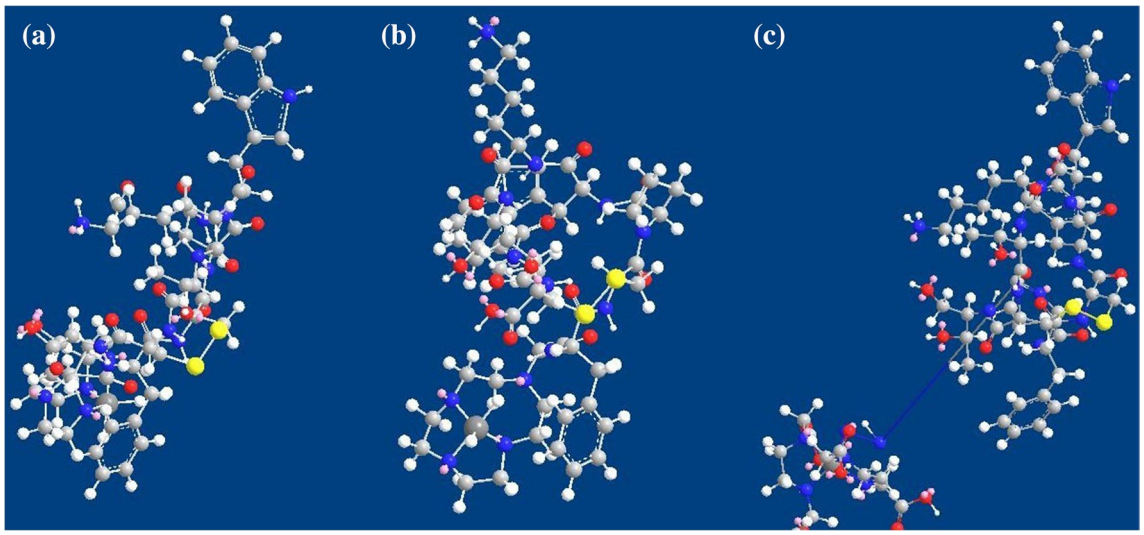

Fig. 4 **a** MM2 energy minimized structure of ^{99m}Tc-HYNIC-AATE. **b** MM2 energy minimized structure of ^{99m}Tc-HYNIC-PATE. **c** MM2 energy minimized structure of ^{99m}Tc-HYNIC-TOC

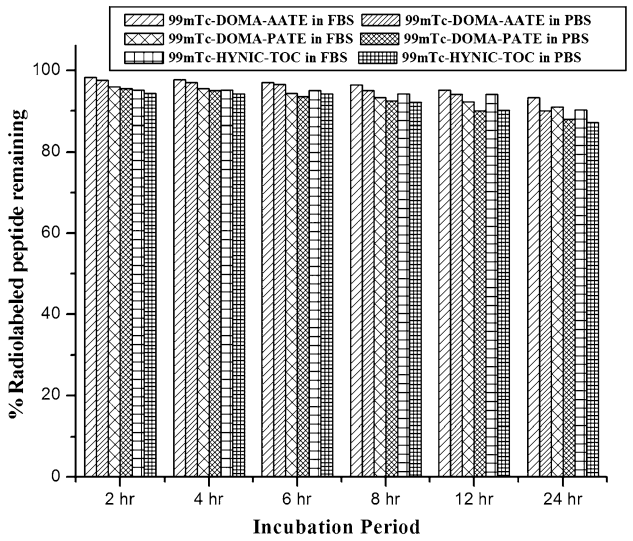

Fig. 5 In vitro stability of ^{99m}Tc-DOMA-AATE, ^{99m}Tc -DOMA-PATE and ^{99m}Tc-HYNIC-TOC in PBS, FBS after incubation at 2–24 h at 37 °C. Data were expressed as the mean ± SD

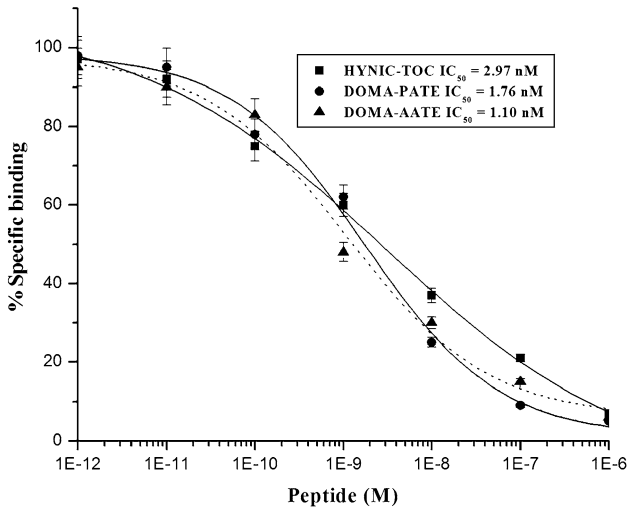

Fig. 6 Competitive inhibition curve of ^{99m}Tc-HYNIC-TOC from somatostatin-binding sites by DOMA-AATE, DOMA-PATE and HYNIC-TOC in C6 cell membrane homogenates

3.17 ± 0.17, 1.40 ± 0.13 and for ^{99m}Tc-DOMA-PATE was 2.17 ± 0.11, 3.95 ± 0.21, 3.10 ± 0.17, 2.10 ± 0.13 at 10, 30, 60 and 120 min (PI). Almost similar trend such as 2.12 ± 0.11, 3.72 ± 0.21, 3.30 ± 0.17 and 2.70 ± 0.13 at 10, 30, 60 and 120 min PI was observed for ^{99m}Tc-HYNIC-TOC in the biodistribution studies in C6 glioma tumor-bearing rat. Blood clearance was very rapid for the radiotracer ^{99m}Tc-DOMA-AATE, ^{99m}Tc-DOMA-PATE and ^{99m}Tc-HYNIC-TOC with blood values as low as 0.22, 0.35 and 0.50 %ID/g as early as 1 h post-administration.

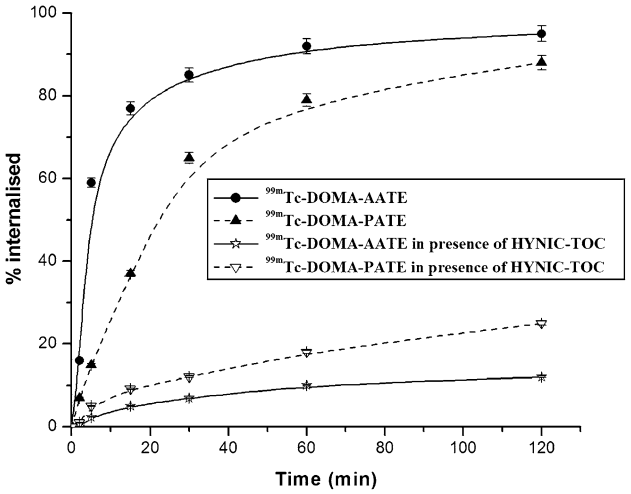

Fig. 7 Internalization of ^{99m}Tc-DOMA-AATE, ^{99m}Tc-DOMA-PATE in C6 cells at 37 °C for various time intervals. Non-specific internalization is also presented here

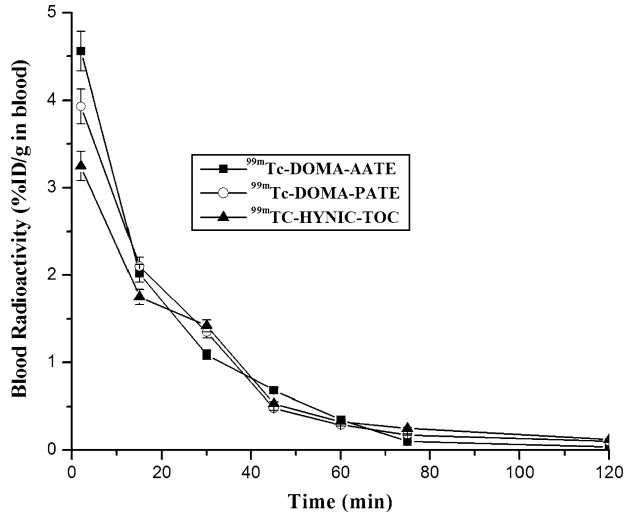

Fig. 8 Blood clearance *curve* of ^{99m}Tc-DOMA-AATE ($n = 5$), ^{99m}Tc-DOMA-PATE ($n = 5$) and ^{99m}Tc-HYNIC-TOC ($n = 5$)

The radioactivity was also rapidly cleared from muscle and other non-target tissues, mainly via the kidneys and the urinary system for the radiotracers. There was relatively low uptake in liver for ^{99m}Tc-DOMA-AATE (0.44 ± 0.03, 0.23 ± 0.13, 0.18 ± 0.12, 0.11 ± 0.03) and ^{99m}Tc-DOMA-PATE (0.40 ± 0.03, 0.52 ± 0.13, 0.28 ± 0.12, 0.17 ± 0.03) but ^{99m}Tc-HYNIC-TOC showed some uptake (0.75 ± 0.03, 0.69 ± 0.13, 0.56 ± 0.12, 0.32 ± 0.03) at 5, 30, 60 and 120 min PI. Quite low uptake of ^{99m}Tc-DOMA-AATE was also observed in stomach (0.33 ± 0.02, 0.60 ± 0.04, 0.40 ± 0.02, 0.25 ± 0.01) at all the time intervals (5, 30, 60 and 120 min), indicating minimal in vivo decomposition of the chelate to form free $^{99m}TcO_4^-$/$^{99m}TcO_2$. Although

Table 2 Biodistribution data of ^{99m}Tc-DOMA-AATE, ^{99m}Tc-DOMA-PATE and ^{99m}Tc-HYNIC-TOC in C6 glioma tumor-bearing rats at 10, 30, 60, and 120 min post-injection (PI) with or without a co-administration of blocking peptide (HYNIC-TOC)

Organ	Time after intravenous injection of radiolabeled peptide				
	10 min	30 min	60 min	60 min blocked	120 min
^{99m}Tc-DOMA-AATE					
Blood	0.54 ± 0.01	0.85 ± 0.01	0.22 ± 0.04	0.23 ± 0.01	0.15 ± 0.01
Liver	0.44 ± 0.03	0.23 ± 0.13	0.18 ± 0.12	0.20 ± 0.03	0.11 ± 0.03
Heart	0.91 ± 0.03	0.77 ± 0.02	0.35 ± 0.02	0.29 ± 0.11	0.15 ± 0.04
Lung	0.87 ± 0.14	0.62 ± 0.03	0.50 ± 0.02	0.52 ± 0.02	0.35 ± 0.11
Kidney	1.97 ± 0.11	3.88 ± 0.21	3.17 ± 0.17	3.18 ± 0.20	1.40 ± 0.13
Intestine	1.21 ± 0.06	1.46 ± 0.05	1.85 ± 0.21	1.36 ± 0.23	0.70 ± 0.05
Spleen	0.54 ± 0.04	0.46 ± 0.01	0.30 ± 0.01	0.33 ± 0.03	0.12 ± 0.02
Pancreas	2.78 ± 0.11	4.20 ± 0.03	2.91 ± 0.06	1.52 ± 0.02	1.22 ± 0.04
Stomach	0.33 ± 0.02	0.60 ± 0.04	0.40 ± 0.02	0.37 ± 0.10	0.25 ± 0.01
Muscle	0.22 ± 0.04	0.16 ± 0.01	0.13 ± 0.03	0.14 ± 0.01	0.09 ± 0.02
C6 tumor	1.08 ± 0.01	1.65 ± 0.01	1.48 ± 0.02	0.54 ± 0.20	1.12 ± 0.03
Urine + urinary bladder	0.61 ± 0.04	2.80 ± 0.01	3.75 ± 0.11	3.72 ± 0.07	4.48 ± 0.22
^{99m}Tc-DOMA-PATE					
Blood	0.42 ± 0.01	0.81 ± 0.01	0.35 ± 0.03	0.38 ± 0.01	0.23 ± 0.00
Liver	0.40 ± 0.03	0.52 ± 0.13	0.28 ± 0.12	0.25 ± 0.03	0.17 ± 0.03
Heart	0.73 ± 0.03	0.67 ± 0.02	0.25 ± 0.02	0.27 ± 0.11	0.09 ± 0.04
Lung	1.07 ± 0.14	0.82 ± 0.03	0.70 ± 0.02	0.78 ± 0.02	0.25 ± 0.11
Kidney	2.17 ± 0.11	3.95 ± 0.21	3.10 ± 0.17	3.18 ± 0.20	2.10 ± 0.13
Intestine	0.90 ± 0.06	1.60 ± 0.05	2.05 ± 0.21	1.56 ± 0.23	0.82 ± 0.05
Spleen	0.62 ± 0.04	0.56 ± 0.01	0.24 ± 0.01	0.26 ± 0.03	0.17 ± 0.02
Pancreas	2.88 ± 0.11	3.49 ± 0.03	2.75 ± 0.06	1.98 ± 0.02	1.10 ± 0.04
Stomach	0.47 ± 0.02	0.91 ± 0.04	0.76 ± 0.02	0.63 ± 0.10	0.20 ± 0.01
Muscle	0.34 ± 0.04	0.20 ± 0.04	0.14 ± 0.03	0.13 ± 0.01	0.10 ± 0.02
C6 tumor	0.80 ± 0.01	1.52 ± 0.01	1.33 ± 0.02	0.72 ± 0.10	0.92 ± 0.03
Urine + urinary bladder	0.47 ± 0.04	2.25 ± 0.01	3.42 ± 0.11	3.45 ± 0.07	4.11 ± 0.22
^{99m}Tc-HYNIC-TOC					
Blood	0.74 ± 0.01	0.75 ± 0.01	0.50 ± 0.04	0.54 ± 0.01	0.35 ± 0.01
Liver	0.75 ± 0.03	0.69 ± 0.13	0.56 ± 0.12	0.20 ± 0.03	0.32 ± 0.03
Heart	1.02 ± 0.03	0.81 ± 0.02	0.47 ± 0.02	0.29 ± 0.11	0.17 ± 0.04
Lung	0.95 ± 0.14	0.77 ± 0.03	0.56 ± 0.02	0.52 ± 0.02	0.32 ± 0.11
Kidney	2.12 ± 0.11	3.72 ± 0.21	3.30 ± 0.17	3.38 ± 0.20	2.70 ± 0.13
Intestine	0.64 ± 0.06	0.42 ± 0.05	0.28 ± 0.21	1.36 ± 0.23	0.12 ± 0.05
Spleen	0.94 ± 0.04	0.51 ± 0.01	0.32 ± 0.01	0.33 ± 0.03	0.26 ± 0.02
Pancreas	2.58 ± 0.11	1.79 ± 0.03	1.11 ± 0.06	0.92 ± 0.02	0.69 ± 0.04
Stomach	0.50 ± 0.02	0.80 ± 0.04	0.72 ± 0.02	0.77 ± 0.10	0.55 ± 0.01
Muscle	0.42 ± 0.10	0.25 ± 0.02	0.19 ± 0.03	0.17 ± 0.01	0.11 ± 0.02
C6 tumor	0.68 ± 0.01	1.25 ± 0.01	1.05 ± 0.02	0.90 ± 0.20	0.87 ± 0.03
Urine + urinary bladder	0.81 ± 0.04	2.15 ± 0.01	3.19 ± 0.11	3.24 ± 0.07	4.10 ± 0.22

All the data represent %ID/g (mean ± SD) value and are the mean of results from five animals per time point

no striking differences in biodistribution studies were observed between ^{99m}Tc-DOMA-AATE, ^{99m}Tc-DOMA-PATE (Table 2) and ^{99m}Tc-HYNIC-TOC (Table 2), the overall ^{99m}Tc-DOMA-AATE and ^{99m}Tc-DOMA-PATE cleared more efficiently ($p < 0.05$) from background tissues and kidneys than ^{99m}Tc-HYNIC-TOC.

In case of somatostatin receptor-rich organs, such as the pancreas, the gastrointestinal tract and C6 tumor ^{99m}Tc-DOMA-AATE, ^{99m}Tc-DOMA-PATE and ^{99m}Tc-HYNIC-TOC exhibited high uptake than other organs. Again ^{99m}Tc-DOMA-AATE and ^{99m}Tc-DOMA-PATE displayed significantly ($p < 0.05$) higher kidney uptake values than ^{99m}Tc-HYNIC-TOC during the initial time intervals and ^{99m}Tc-HYNIC-TOC showing slower washout from the kidney and background tissues over 2 h post-injection. These organ uptakes were also shown to be receptor

specific, as significant reduction ($p < 0.01$) of the uptake (Table 2) in the group of blocked animals (receiving 100 μg HYNIC-TOC) was observed. The reduction was >70 % in the C6 glioma tumor and >45 % in the case of pancreas. No blocking was found in the liver, the kidneys or the spleen and was, therefore, considered to be receptor-mediated process. For example, the pancreas uptake of 2.91 ± 0.06 % ID/g for ^{99m}Tc-DOMA-AATE, 2.75 ± 0.06 % ID/g ^{99m}Tc-DOMA-PATE at 60 min post-administration reached only 1.52 ± 0.02 and 1.98 ± 0.02 %ID/g, respectively, in the group of blocked animals. Again C6 tumor uptake of 1.48 ± 0.02 %ID/g for ^{99m}Tc-DOMA-AATE and 1.33 ± 0.02 %ID/g for ^{99m}Tc-DOMA-PATE at 60 min and significant ($p < 0.01$) reduction in tumor uptake (0.54 ± 0.20 %ID/g for ^{99m}Tc-DOMA-AATE and 0.72 ± 0.10 %ID/g for ^{99m}Tc-DOMA-PATE) was observed in the blocked animals. No appreciable differences were observed for non-somatostatin receptor-positive organs between rats that received a co-injection of blocking dose and unblocked rats. Accumulation of ^{99m}Tc-DOMA-AATE, ^{99m}Tc-DOMA-PATE and ^{99m}Tc-HYNIC-TOC in the C6 glioma tumor did not show significant differences during the very initial time points but at 30 min post-injection ^{99m}Tc-DOMA-AATE and ^{99m}Tc-DOMA-PATE displayed significantly ($p < 0.05$) higher uptake values than ^{99m}Tc-HYNIC-TOC. However, after 2 h post-administration, kidney uptake values for ^{99m}Tc-HYNIC-TOC were found to be higher than those for the ^{99m}Tc-DOMA-AATE, ^{99m}Tc-DOMA-PATE. This is due to a greater degree of retention and slower wash out of ^{99m}Tc-HYNIC-TOC from the kidney and other background tissues compared to ^{99m}Tc-DOMA-AATE, ^{99m}Tc-DOMA-PATE. Some important tumor to normal tissue ratios are also given in Fig. 9. The higher tumor to blood ratios were found at 30 min post-injection for both the radiotracers ^{99m}Tc-DOMA-AATE and ^{99m}Tc-DOMA-PATE. As the background activity gradually cleared from the body, there was increase in target to non-target ratios with the passage of time. Here tumor to blood ratios of ^{99m}Tc-DOMA-AATE, ^{99m}Tc-DOMA-PATE and ^{99m}Tc-HYNIC-TOC were 2.29, 1.87 and 1.66, and tumor to muscle ratios were 10.31, 7.6 and 5.01, which were high while tumor to kidney ratios were (0.50, 0.38 and 0.30) low at 30 min post-administration. These radiolabeled peptides ^{99m}Tc-DOMA-AATE, ^{99m}Tc-DOMA-PATE and ^{99m}Tc-HYNIC-TOC were excreted mainly through the renal routes. The clearance of activity through this path was as fast as can be observed from the accumulation of large amount of activity in the urinary bladder. The urinary excretion was comparatively less in case of ^{99m}Tc-HYNIC-TOC than ^{99m}Tc-DOMA-AATE and ^{99m}Tc-DOMA-PATE. The excretion results demonstrated that ^{99m}Tc-HYNIC-AATE (Table 2) was cleared more rapidly from the blood, heart, lung and muscle into the urine via the kidneys and the urinary tract as a result of its high hydrophilicity (log $p = -1.70 \pm 0.12$) than ^{99m}Tc-DOMA-PATE (log $p = -1.62 \pm 0.10$) and ^{99m}Tc-HYNIC-TOC (log $p = -1.15 \pm 0.04$).

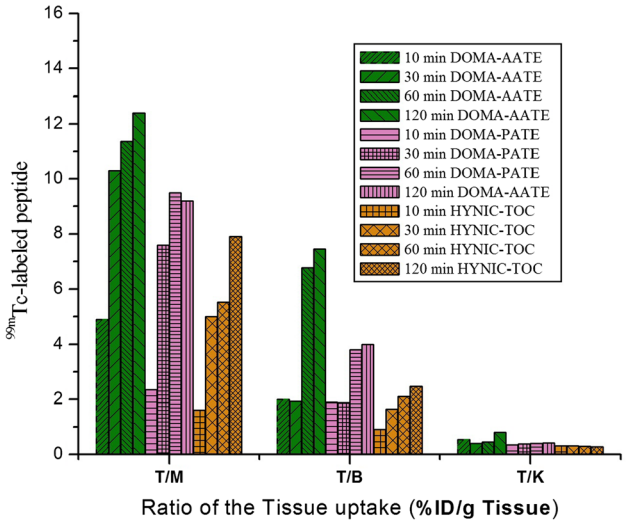

Fig. 9 Comparative tumor to non-target tissue ratios of ^{99m}Tc-DOMA-AATE, ^{99m}Tc-DOMA-PATE and ^{99m}Tc-HYNIC-TOC in C6 glioma tumor-bearing rats at 10, 30, 60 and 120 min post-injection. Tumor to muscle (*T/M*), tumor to blood (*T/B*) and tumor to kidneys (*T/K*). All the data represent %ID/g values and are the mean of results from five animals per time point

Imaging studies

Scintigraphic images allow a direct comparison between different organs for their imaging quality in living animals. To further demonstrate the biological performance of ^{99m}Tc-DOMA-AATE, ^{99m}Tc-DOMA-PATE and ^{99m}Tc-HYNIC-TOC complexes, the imaging studies of radiotracers in glioma tumor-bearing rats (Fig. 10g) under anesthesia were performed (nine animals have been used for imaging studies). Figure 10a–c shows the images of C6 tumor-bearing SD rats, 30 min post-administration of ^{99m}Tc-DOMA-AATE, ^{99m}Tc-DOMA-PATE and ^{99m}Tc-HYNIC-TOC with and without a co-injected blocking dose of HYNIC-TOC. High uptake in the rat C6 tumors was visible at 30 min post-injection of ^{99m}Tc-DOMA-AATE, ^{99m}Tc-DOMA-PATE and ^{99m}Tc-HYNIC-TOC. Conversely, the other rat that received a blocking dose showed reduced uptake at thigh C6 tumor sites (Fig. 10a′–c′). Prominent uptake was observed in the kidneys in all animals. 1 h after administration of ^{99m}Tc-DOMA-AATE, ^{99m}Tc-DOMA-PATE and ^{99m}Tc-HYNIC-TOC (Fig. 10d–f), tumor site in the non-blocked animal could still be easily identified, as well as showing higher uptake than other normal organs. Owing to the high tumor uptake and

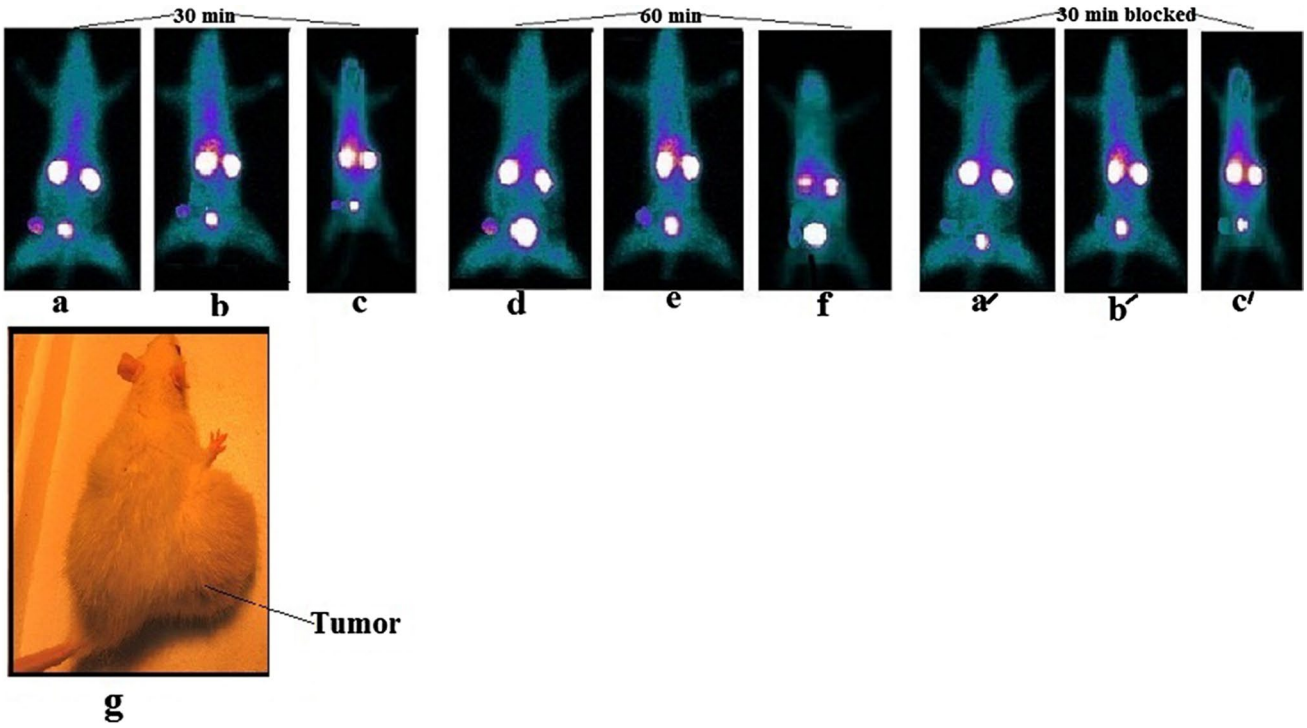

Fig. 10 Planner static images of C6 tumor-bearing rat at different time period after i.v. injection of **a** ^{99m}Tc-DOMA-AATE alone at 30 min, **b** ^{99m}Tc-DOMA-PATE alone at 30 min, **c** ^{99m}Tc-HYNIC-TOC alone at 30 min, **d** ^{99m}Tc-DOMA-AATE alone at 60 min, **e** ^{99m}Tc-DOMA-PATE alone at 60 min, **f** ^{99m}Tc-HYNIC-TOC alone at 60 min. **a′** ^{99m}Tc-DOMA-AATE blocked by co-injection of HYNIC-TOC at 30 min. **b′** ^{99m}Tc-DOMA-PATE blocked by co-injection of HYNIC-TOC at 60 min. **c′** ^{99m}Tc-HYNIC-TOC blocked by co-injection of HYNIC-TOC at 60 min. **g** Tumor developed in rats after 21 days of subcutaneous injection of C6 glioma cell into flank of 6-week-old SD rats

fast renal excretion, the accumulation of radioactivity for tumors to muscle ratios was high and low for tumor to kidney ratios at 30 min post-injection of ^{99m}Tc-DOMA-AATE, ^{99m}Tc-DOMA-PATE and ^{99m}Tc-HYNIC-TOC demonstrating no statistical difference between biodistribution and scintigraphic studies. The tumors were clearly visualized at 30 min post-injection with excellent tumor to background contrast due to significant amount of radioactivity associated with SSTR2-positive C6 tumor. The other most prominent regions of ^{99m}Tc-DOMA-AATE, ^{99m}Tc-DOMA-PATE and ^{99m}Tc-HYNIC-TOC uptakes were the kidneys and bladder, due to rapid excretion of these compounds into the urine via kidney. As shown by the static images, significant tumor uptake and excellent clearing properties of ^{99m}Tc-DOMA-AATE from the background tissues and kidney compared to ^{99m}Tc-DOMA-PATE and ^{99m}Tc-HYNIC-TOC are evident in the C6 tumor-bearing animals at 30 min and 60 min post-administration (Fig. 10). All these image results are in concurrence with the biodistribution results of the ^{99m}Tc-DOMA-AATE, ^{99m}Tc-DOMA-PATE and ^{99m}Tc-HYNIC-TOC in C6 tumor-bearing rats.

Discussion

Solid-phase synthesis of a wide variety of biologically active small synthetic peptides radiolabeled with ^{99m}Tc for diagnosis of various diseases has opened a new era in the field of nuclear medicine (Bakker et al. 1991; de Jong et al. 1998). The goal of this research was to design stable ^{99m}Tc-labeled new somatostatin analogs which have great potential for imaging receptor-specific tumor and to compare with ^{99m}Tc-HYNIC-TOC. Here in this study, two new octapeptides were synthesized where C-terminal alcohol of octreotide was replaced with a C-terminal acid (TATE) and chelating agent DOMA was conjugated as an N-terminal ligand of Asn^3-octreotate and Pro3-octreotate, expected to increase the hydrophilicity and thereby show better in vivo performance of final ^{99m}Tc-DOMA-AATE and ^{99m}Tc-DOMA-PATE radioligand than known octreotide ^{99m}Tc-HYNIC-TOC. It was also expected that modification of Tyr3-octreotide by the use of Asn^3 and Pro^3 amino acids in place of Tyr^3 of octreotide and conjugation with DOMA chelating agent may enhance their excretion through renal pathway.

In our study, two new octapeptides were synthesized successfully and then conjugated with DOMA with more than 95 % pure yield and labeled with ^{99m}Tc with a high efficiency as single radiochemical products. A particular convenient feature was that the DOMA was added with peptide still attached to support. The radiocomplexes were substantially stable up to 24 h when incubated with PBS and serum. The in vitro C6 cell binding and % internalization of radioactivity and in vivo biodistribution studies of C6 tumor-bearing rats were also measured for these ^{99m}Tc octapeptides (^{99m}Tc-DOMA-AATE, ^{99m}Tc-DOMA-PATE and ^{99m}Tc-HYNIC-TOC). The internalization observed in the present study was rather fast and high in case of ^{99m}Tc-DOMA-AATE, ^{99m}Tc-DOMA-PATE compared to ^{99m}Tc-HYNIC-TOC. Receptor-binding experiments using C6 glioma tumor membranes were performed to compare the IC_{50} values of ^{99m}Tc-DOMA-AATE, ^{99m}Tc-DOMA-PATE and ^{99m}Tc-HYNIC-TOC. In our study, we found that affinity binding of the complexes was in the nanomolar range, in C6 glioma cell membranes which mostly express SSTR2 (Lamszus et al. 1997; Barbieri and Florio 2011; Vaidyanathan et al. 2003; Reubi et al. 2001). Our data showed that among three radiocomplexes ^{99m}Tc-DOMA-AATE has a highest potential to bind and internalize in tumor cells with SSTR2 expression than ^{99m}Tc-DOMA-PATE and after that ^{99m}Tc-HYNIC-TOC.

In C6 tumor-bearing rats, biodistribution of ^{99m}Tc-DOMA-AATE, ^{99m}Tc-DOMA-PATE and ^{99m}Tc-HYNIC-TOC has shown high and receptor-mediated uptake in the tumor as well as in the SSTR2-positive tissues. The bulk of radioactivity was rapidly excreted from the body into the urine via the kidneys and the urinary system. Among all three radiopeptides, ^{99m}Tc-DOMA-AATE cleared more rapidly from background tissues, presumably as a result of its higher hydrophilicity (hydrophilicity sequence were ^{99m}Tc-DOMA-AATE > ^{99m}Tc-DOMA-PATE > ^{99m}Tc-HYNIC-TOC). Their respective HPLC profiles under identical chromatographic conditions revealed the higher hydrophilic character of ^{99m}Tc-DOMA-AATE than ^{99m}Tc-DOMA-PATE and ^{99m}Tc-HYNIC-TOC. While the general biodistribution pattern again seems very similar for the three tracers, a few significant differences can be pointed out. Firstly during the initial time intervals (30 min), ^{99m}Tc-DOMA-AATE and ^{99m}Tc-DOMA-PATE showed significantly higher radioactivity uptake and good retention in the tumor and the SSTR2-positive tissues, like the pancreas and intestines than ^{99m}Tc-HYNIC-TOC. In contrast after 2 h post-injection, most of the ^{99m}Tc-DOMA-AATE and ^{99m}Tc-DOMA-PATE radioactivities have washed out significantly much faster from these tissues as compared to the ^{99m}Tc-HYNIC-TOC. It is interesting to note that the radioactivity distribution pattern of ^{99m}Tc-DOMA-AATE, ^{99m}Tc-DOMA-PATE and ^{99m}Tc-HYNIC-TOC within the rat kidney was very similar in the initial time periods. These findings imply a common course of radioactivity through kidney of the rat, which was previously described for other radiolabeled somatostatin analogs (De et al. 2012). The faster renal washout observed in the case of ^{99m}Tc-DOMA-AATE and ^{99m}Tc-DOMA-PATE at the longer time intervals (after 2 h post-injection) is reminiscent of its behavior in the experimental tumor and in the physiological SSTR2-positive sites and contrasts with the prolonged residence of ^{99m}Tc-HYNIC-TOC in these tissues. We know from the previous literature that the molecular charges of peptide play an important role in re-absorption of the protein from glomerular filtrate into renal proximal tubular cells (Kopecky et al. 2004; Laznickova et al. 2002). However, since negatively charged ^{99m}Tc-DOMA/^{99m}Tc-HYNIC is attached to these peptides and changed one amino acid that significantly altered the net charges of the resulting octreotide derivative than TOC. Due to this, all the radiolabeled peptides showed rapid clearance from the blood after administration. The major radioactivity was excreted to urine as intact forms after administration of the radio peptides. While a shorter residence of radioactivity in the kidney is highly desirable, therapy can only benefit from it if retention in the tumor is not compromised. The present study also shows a high and persistent uptake of this radioligand for the tumor and a low uptake for the liver and other SSTR2-negative organs. The results of the blocking experiment revealed that these uptakes were specific, and receptor mediated. Except for kidneys, which are the main organs of excretion, very fast clearance of this tracer from all SSTR2-negative tissues of the body via the kidneys into the bladder was observed. As a result, high target to background ratios were exhibited by ^{99m}Tc-DOMA-AATE followed by ^{99m}Tc-DOMA-PATE, illustrating the favorable characteristics of this agent for tumor imaging. During scintigraphic studies, tumor region was also clearly visible in the case of two new radiocomplexes. All these properties were clearly evident that ^{99m}Tc-DOMA-AATE and ^{99m}Tc-DOMA-PATE have SSTR2 expressing C6 glioma tumor localization properties and comparing all imaging properties of these labeled peptides, ^{99m}Tc-DOMA-AATE is most receptor specific tumor targeting agents than the ^{99m}Tc-DOMA-PATE and ^{99m}Tc-HYNIC-TOC.

Conclusion

The study presented here demonstrates that two new radiopeptides, ^{99m}Tc-DOMA-AATE and ^{99m}Tc-DOMA-PATE, have shown in general high uptake in SSTR2-positive C6 tumor which is required for imaging purpose. But the radiopeptide ^{99m}Tc-DOMA-AATE has shown significantly higher uptake in the SSTR2-positive C6 tumor in the rat

with lower background activity and also has faster clearance from the non-target tissues than ^{99m}Tc-DOMA-PATE and ^{99m}Tc-HYNIC-TOC. Due to faster blood clearance and rapid urinary excretion, ^{99m}Tc-DOMA-AATE exhibited gradual increase in tumor muscle and tumor blood ratios over the period of study, making it suitable for nuclear medicine application. Its potential usefulness as a diagnostic agent is currently being compared directly and in detail with that of ^{99m}Tc-HYNIC-TOC. In view of this study, ^{99m}Tc-DOMA-AATE acts as a good ^{99m}Tc-radiotracer for targeted imaging of SSTR2-positive tumor and seems a very promising candidate for the scintigraphic detection of SSTR2-positive lesions in the clinical phase. In the light of the results presented here, it is our further aim to prepare new radiolabeled receptor-specific peptides conjugated to chelates to be used in nuclear medicine applications.

Acknowledgments Financial support in the form of Research Associateship (Dr. Kakali De) from the Indian Council of Medical Research (ICMR), New Delhi, India, is acknowledged. The authors also gratefully acknowledge Prof. Siddhartha Roy, Director, CSIR-Indian Institute of Chemical Biology, Kolkata, India for providing infrastructure facilities. Authors sincerely acknowledge Dr. Santanu Ganguly and Mr. Bhart Sarkar of Regional Radiation Medicine Centre and Variable Energy Cyclotron Centre, Thakurpukur Cancer Centre and Welfare Home Campus, Kolkata, India, for their kind help for taking the image of tumor-bearing rats.

Conflict of interest The authors declare that they have no conflict of interests.

References

Arnold R, Simon B, Wied M (2000) Treatment of neuroendocrine GEP tumors with somatostatin analogs: a review. Digestion 62:84–91

Babich JW, Fischman AJ (1995) Effect of Co-ligand on the biodistribution of ^{99m}Tc-labeled hydrazine nicotinic acid derivatized chemotactic peptides. Nucl Med Biol 22:25–30

Bakker WH, Albert R, Bruns C, Breeman WAP, Hofland LJ, Marbach P, Pless J, Pralet D, Stolz B, Koper JW, Lamberts SWJ, Visser TJ, Krenning EP (1991) In-111-DTPA-D-Phe1-octreotide, a potential radiopharmaceutical for imaging of somatostatin receptor-positive tumors-synthesis, radiolabeling and invitro validation. Life Sci 49(22):1583–1591

Barbieri F, Florio T (2011) Characterization of the differential efficacy of somatostatin receptor agonists in the inhibition of the growth of experimental gliomas and identification of the intracellular mechanisms involved. Eur J Clin Med Oncol 3:46–53

Behera A, De K, Chandra S, Chattopadhyay S, Misra M (2011) Synthesis, radiolabelling and biodistribution of HYNIC-Tyr3 octreotide: a somatostatin receptor positive tumour imaging agent. J Radioanal Nucl Chem 290(1):123–129

De Jong M, Breeman WAP, Bernard BF, Hofland LJ, Srinivasan TJ, Schmidt M, Behe M, Maecke H, Krenning PE (1998) Preclinical comparison of [DTPA^0] octreotide, [DTPA^{0}Tyr^3] octreotide and [DOTA^{0}Tyr^3] octreotide as carriers for somatostatin receptor targeted scintigraphy and radionuclide therapy. Int J Cancer 75:406–411

De K, Chadra S, Sarkar B, Ganguly S, Misra M (2010) Synthesis and biological evaluation of ^{99m}Tc-DHPM complex : a potential new radiopharmaceutical for lung imaging studies. J Radioanal Nucl Chem 283:621–628

De K, Bhowmik A, Behera A, Banerjee I, Ghosh MK, Misra M (2012) Synthesis, radiolabeling and preclinical evaluation of a new octreotide analog for somatostatin receptor-positive tumor scintigraphy. J Pept Sci 18:720–730

Decristoforo C, Mather JS (1999) Preparation, ^{99m}Tc-labeling, and in vitro characterization of HYNIC and N_3S modified RC-160 and [Tyr^3] octreotide. Bioconj Chem 19:431–438

Decristoforo C, Melendez-Alafort L, Sosabowski JK, Mather SJ (2000) 99mTc-HYNIC-[Tyr3]-octreotide for imaging somatostatin-receptor-positive tumors: preclinical evaluation and comparison with 111In-octreotide. J Nucl Med 41(6):1114–1119

Fischman AJ, Babich JW, Strauss HW (1993) A ticket to ride : peptide radiopharmaceuticals. J Nucl Med 34(12):2253–2263

Gandomkar M, Najafi R, Shafiei M, Mazidi M, Ebrahimi SES (2007) Preclinical evaluation of Tc-99m/EDDA/tricine/HYNIC0,1-Nal(3), Thr(8)-octreotide as a new analogue in the detection of somatostatin-receptor-positive tumors. Nucl Med Biol 34(6):651–657

Graham MM, Menda Y (2011) Radiopeptide imaging and therapy in the United States. J Nucl Med 52:56S–63S

Guggenberg EV, Penz B, Kemmler G, Virgolini I, Decristoforo C (2006) Comparison of different methods for radiochemical purity testing of [Tc-99m-EDDA-HYNIC-D-Phe(1), Tyr(3)]-octreotide. Appl Radiat Isot 64:194–200

Hanaoka H, Tominaga H, Yamada K, Paudyal P, Iida Y, Watanabe S, Paudyal B, Higuchi T, Oriuchi N, Endo K (2009) Evaluation of 64CU-labeled DOTA-D-Phe1-Tyr3-octreotide(64Cu-DOTA-TOC) for imaging somatostatin receptor-expressing tumors. Ann Nucl Med 23:559–567

Koenig JA, Edwardson JM, Humphrey PPA (1997) Somatostatin receptors in Neuro2A neuroblastoma cells: operational characteristics. Br J Pharmacol 120(1):45–51

Kopecky M, Semecky V, Trejtnar F, Laznicek M, Laznickova A, Nachtigal P (2004) Analysis of accumulation of ^{99m}Tc-octreotide and ^{99m}Tc-EDDA/HYNIC-Tyr3-octreotide in the rat kidneys. Nucl Med Biol 31:231–239

Kwekkeboom DJ, Krenning EP (2002) Somatostatin receptor imaging. Semin Nucl Med 32:84–91

Lamszus K, Meverhof W, Westpha M (1997) Somatostatin and somatostatin receptors in the diagnosis and treatment of gliomas. J Neuro Oncol 35:353–364

Laznickova A, Laznicek M, Trejtnar F, Melicharova L, Suzuki KH, Akizawa H, Arano Y, Yokoyama A (2002) Distribution and elimination characteristics of 111In-DTPA-D-Phe1-octreotide and 111In-DTPA-L-Phe1-octreotide in rats. Eur J Drug Metab Pharmacokin 27:37–43

Lee TW, Chang SR, Chen ST, Tsai ZT (1998) Convenient solid-phase synthesis of tyr(3)-octreotide. Appl Radiat Isot 49(12):1581–1586

Li WP, Lewis JS, Kim J, Bugaj JE, Johnson MA, Erion JL, Anderson CJ (2002) DOTA-D-Tyr^1-octreotate: a somatostatin analogue for labeling with metal and halogen radionuclides for cancer imaging and therapy. Bioconj Chem 13:721–728

Liu S, Edwards DS (1999) Tc-99m-labeled small peptides as diagnostic radiopharmaceuticals. Chem Rev 99(9):2235–2268

Maina T, Nock BA, Cordopatis P, Bernard BF, Breeman WAP, van Gameren A, van den Berg R, Reubi JC, Krenning EP, de Jong M (2006) Tc-99m demotate 2 in the detection of sst(2)-positive tumours: a preclinical comparison with In-111 DOTA-tate. Eur J Nucl Med Mol Imaging 33(7):831–840

Nikolopoulou A, Nock BA, Maina T (2006) Tc-99m targeting of Sst(2)-expressing tumors by tetraamine-octreotide: first results in CA20948 cells and rat models. Anticancer Res 26(1A):363–366

Okarvi SM (2004) Peptide-based radiopharmaceuticals: future tools for diagnostic imaging of cancers and other diseases. Med Res Rev 24:357–397

Panwar P, Iznaga-Escobar N, Mishra P, Srivastava V, Sharma RK, Chandra R, Mishra AK (2005) Radiolabeling and biological evaluation of DOTA-Ph-Al derivative conjugated to anti-egfr antibody ior egf/r3 for targeted tumor imaging and therapy. Cancer Biol Ther 4:854–860

Reubi JC, Waser B, Schaer JC, Laissue JA (2001) Somatostatin receptor sst1-sst5 expression in normal and neoplastic human tissues using receptor autoradiography with subtype-selective ligands. Eur J Nucl Med 28(7):836–846

Storch D, Behe M, Walter MA, Chen JH, Powell P, Mikolajczak R, Macke HR (2005) Evaluation of Tc-99m/EDDA/HYNIC0 octreotide derivatives compared with In-111-DOTA(0), Tyr(3), Thr(8) octreotide and In-111-DTPA(0) octreotide: does tumor or pancreas uptake correlate with the rate of internalization? J Nucl Med 46(9):1561–1569

Susini C, Buscail L (2006) Rational for the use of somatostatin analogs as antitumor agents. Ann Oncol 17:1733–1742

Vaidyanathan G, Friedman HS, Affleck DJ, Schottelius M, Wester HJ, Zalutsky MR (2003) Specific and high-level targeting of radiolabeled octreotide analogues to human medulloblastoma xenografts. Clin Cancer Res 9(5):1868–1876